

Soft Materials

How to cite: *Angew. Chem. Int. Ed.* **2021**, *60*, 11604–11627

International Edition: doi.org/10.1002/anie.202007693

German Edition: doi.org/10.1002/ange.202007693

Self-Assembly of Photoresponsive Molecular Amphiphiles in Aqueous Media

Shaoyu Chen, Romain Costil, Franco King-Chi Leung,* and Ben L. Feringa*

Keywords:

aqueous medium ·
photoresponsive amphiphile ·
responsive foam ·
soft material ·
supramolecular
assembly



Angewandte
International Edition
Chemie

Amphiphilic molecules, comprising hydrophobic and hydrophilic moieties and the intrinsic propensity to self-assemble in aqueous environment, sustain a fascinating spectrum of structures and functions ranging from biological membranes to ordinary soap. Facing the challenge to design responsive, adaptive, and out-of-equilibrium systems in water, the incorporation of photoresponsive motifs in amphiphilic molecular structures offers ample opportunity to design supramolecular systems that enables functional responses in water in a non-invasive way using light. Here, we discuss the design of photoresponsive molecular amphiphiles, their self-assembled structures in aqueous media and at air–water interfaces, and various approaches to arrive at adaptive and dynamic functions in isotropic and anisotropic systems, including motion at the air–water interface, foam formation, reversible nanoscale assembly, and artificial muscle function. Controlling the delicate interplay of structural design, self-assembling conditions and external stimuli, these responsive amphiphiles open several avenues towards application such as soft adaptive materials, controlled delivery or soft actuators, bridging a gap between artificial and natural dynamic systems.

1. Introduction

The word amphiphile, derived from the Greek *αμφις*, *amphis*: both and *φιλία*, *philia*: love, refers to chemical compounds that consist of a polar part and a nonpolar moiety with both hydrophilic (water-loving) and lipophilic (fat-loving) properties.^[1–4] Common amphiphiles include surfactants (e.g., detergents) and diglycerides (e.g., phospholipids).^[5] The coexistence of both hydrophobic and hydrophilic moieties in the same small molecular building blocks, i.e., amphiphilic nature of the molecule, allows spontaneous self-assembly into well-defined structures at interfaces and in solution based on non-covalent interactions.^[6–14] The hydrophilic part of an amphiphile interacts with a polar phase and as a result, the hydrophobic component interacts with a non-polar environment or is exposed to air, forming among others self-assembled structures in solution (e.g., micelles and bilayers) or at the air–water interface (e.g., monolayers).^[15,16] It should be noted that amphiphiles, besides being the key components of cell membranes, play a crucial role throughout chemistry and society, providing diverse applications ranging from vesicles for drug delivery, household detergents, and materials for enhanced oil recovery.^[17–22] The bottom-up approach allows to build natural and synthetic supramolecular structures of amphiphiles over multiple length scales.^[15,23–44]

Nature has arguably provided the most elegant examples of self-assembled systems derived from amphiphiles. Phospholipids, a typical class of natural amphiphiles, self-assemble into biological bilayer membranes in living organisms.^[45,46] The presence of proteins, enabling specific functions, endows the living organisms with “smart” self-assembled structures, allowing these membranes to automatically respond to subtle

From the Contents


1. Introduction	11605
2. Photoresponsive molecular amphiphiles	11606
3. Dynamic functions of photoresponsive molecular amphiphiles in Gibbs Monolayers	11607
4. Functional supramolecular self-assembly of photoresponsive molecular amphiphiles in solution	11612
5. Summary and outlook	11622


variations in the surrounding environment.^[15,47] Taking inspiration from Nature, various synthetic supramolecular self-assembled systems are designed and equipped with functional

tunability and responsiveness to enable sophisticated assembling pathways and energy landscapes.^[48–56] Noticeably, a variety of stimuli-responsive synthetic amphiphiles have been designed to develop well-defined supramolecular self-assemblies whose structures can be manipulated by external stimuli such as pH, CO₂, heat, and light.^[8,57–78] The use of light as a non-invasive stimulus offers multiple advantages such as tunable wavelength and intensity as well as high temporal and spatial control.^[79,80] Structural modifications of photoresponsive amphiphilic molecules include intrinsic light-switches and attachment of a photoresponsive unit (photoresponsive molecular amphiphile) or the introduction of a photoresponsive component via noncovalent interactions (photoresponsive supramolecular amphiphile).^[9,67,81] Supramolecular assemblies of photoresponsive amphiphiles controlled by

[*] Dr. S. Chen, Dr. R. Costil, Dr. F. K. C. Leung, Prof. Dr. B. L. Feringa Stratingh Institute for Chemistry, University of Groningen Nijenborgh 4, 9747AG Groningen (Netherlands)
E-mail: b.l.feringa@rug.nl

Dr. F. K. C. Leung
Present address: State Key Laboratory of Chemical Biology and Drug Discovery, Department of Applied Biology and Chemical Technology, The Hong Kong Polytechnic University
Hong Kong (China)
E-mail: kingchifranco.leung@polyu.edu.hk

 The ORCID identification number(s) for the author(s) of this article can be found under <https://doi.org/10.1002/anie.202007693>.

 © 2020 The Authors. Angewandte Chemie International Edition published by Wiley-VCH GmbH. This is an open access article under the terms of the Creative Commons Attribution Non-Commercial License, which permits use, distribution and reproduction in any medium, provided the original work is properly cited and is not used for commercial purposes.

light provide important opportunities towards smart and adaptive materials, and responsive systems in areas ranging from nanotechnology, chemical biology to material science.^[5,79,82,83]

Virtually, all functional supramolecular self-assembly processes found in living systems take place in aqueous media.^[84,85] Water is a critical and unique medium for self-assembly in biological systems, allowing for complexity, adaptability, and robustness. Supramolecular self-assembly of photoresponsive molecular amphiphiles in aqueous media provides attractive opportunities to create biocompatible systems.^[31,42,85] In this context, we discuss recent progress in the field of supramolecular self-assembled structures of photoresponsive small molecular amphiphiles in aqueous media, both at air–water interfaces and in aqueous solutions, including their molecular structures, hierarchical organization, key recognition and self-assembly parameters as well as responsive behavior. The following topics are discussed: (1) molecular design of photoresponsive amphiphiles, (2) dynamic functions of photoresponsive molecular amphiphiles at air–water interfaces, i.e., Gibbs monolayers, and (3) functional supramolecular self-assembly of photoresponsive molecular amphiphiles in solutions, ranging from one-dimensional nanostructures to isotropic entangled three-dimensional networks and anisotropic hierarchical structures. With a focus on structures and functions of photoresponsive molecular amphiphiles and their self-assembly in water, we highlight recent progress in the design of dynamic systems in

water and the amplification of molecular motion to achieve macroscopic responsive functions.

2. Photoresponsive molecular amphiphiles

In order to design photoresponsive amphiphiles, that is, photoswitchable systems (and, where relevant, photocleavable systems), to achieve proper self-assembled structures controlled by light in water, one should take into consideration the various molecular structures of amphiphiles.^[17,86] Based on the chemical nature of the hydrophilic moiety, amphiphiles are commonly classified into ionic (i.e., anionic, cationic), zwitterionic, and nonionic amphiphiles.^[6,17,86] According to the number and mode of connections of the hydrophilic moiety (polar head) and the lipophilic moiety (hydrophobic tail), amphiphiles are also classified as single head/single tail amphiphiles, bolaamphiphiles, gemini amphiphiles, and double tail amphiphiles (Figure 1a).^[4,5,87] Among them, conventional single head/single tail amphiphiles, bolaamphiphiles, and gemini amphiphiles are the common types in both natural and synthetic systems. Bolaamphiphiles containing two hydrophilic head groups connected by a hydrophobic chain are found in the cell membranes of thermophilic bacteria.^[88,89] Bolaamphiphiles usually show high thermal resistance.^[15] Gemini amphiphiles, consisting of two hydrocarbon tails and two ionic groups linked by a spacer, can aggregate at very low concentrations and can also signifi-



Shaoyu Chen obtained her BSc in Textile Chemistry at Jiangnan University in 2013. Afterwards, she continued her master and doctoral study at Jiangnan University under the supervision of Prof. Chaoxia Wang in the field of smart photo-responsive materials. In October 2017, she joined Prof. Feringa's group as a PhD student. After earning her PhD in 2019, she continues to work in Prof. Feringa's group as a Postdoc. Her main research interests are the synthesis and application of photo-responsive materials.



Franco King-Chi Leung studied his BSc in Chemistry at The Hong Kong Polytechnic University where he carried out his Masters research in catalysis and chemical biology under supervision of Prof. Man Kin Wong. He expanded his research scopes in his PhD to supramolecular chemistry and material science under guidance of Prof. Takatori Fukushima in Tokyo Institute of Technology. In 2017, he joined Prof. Ben L. Feringa's group, as a postdoc fellow and later he was awarded the Croucher Postdoctoral Fellow. In 2019, he was appointed as assistant

professor in Department of Applied Biology and Chemical Technology, The Hong Kong Polytechnic University. His main research interests are dynamic supramolecular polymers, functional molecular assembly, and biocompatible functional materials.



Romain Costil studied Organic, Bio-organic and Therapeutic Chemistry at the Ecole Nationale Supérieure de Chimie de Mulhouse in France, where he was awarded a Diplôme d'ingénieur in 2014. During his studies, he worked in Axon MedChem in Groningen, the Netherlands, on the synthesis of drug candidates for commercial use. He then joined the group of Prof. Jonathan Clayden in the United Kingdom for a M.Sc project in foldamer chemistry, followed by a Ph.D. investigating the synthesis and properties of a novel class of atropisomers. After a postdoc in the Feringa lab working on photoswitchable metallo-supramolecular complexes, he is now a research manager in the same group.



Ben L. Feringa obtained his PhD degree in 1978 at the University of Groningen in the Netherlands under the guidance of Prof. Hans Wynberg. After working as a research scientist at Shell he was appointed full professor at the University of Groningen in 1988 and named the distinguished Jacobus H. van't Hoff Professor of Molecular Sciences in 2004. He was elected foreign honorary member of the American Academy of Arts and Sciences and member of the Royal Netherlands Academy of Sciences. His research interests include stereochemistry, organic synthesis, asymmetric catalysis, molecular switches and motors, photopharmacology, self-assembly and nanosystems.

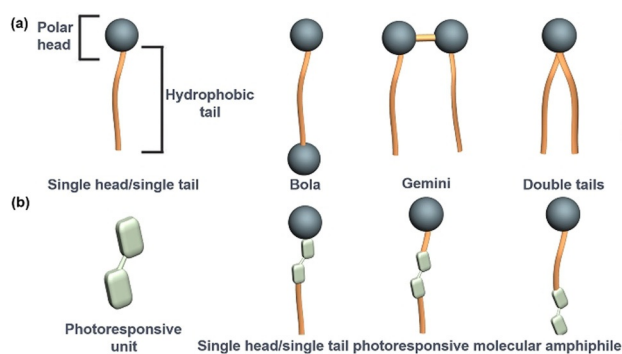
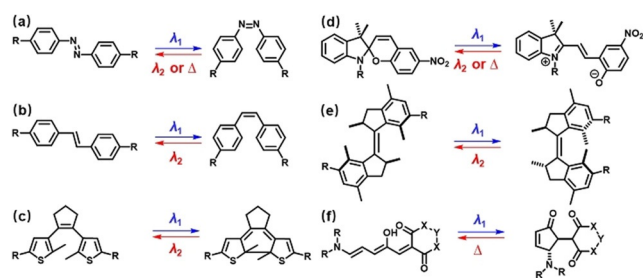


Figure 1. Schematic illustration of (a) typical types of molecular amphiphiles and (b) photoresponsive molecular amphiphiles (taking single head/single tail amphiphiles as an example).

cantly reduce surface tension.^[5,15,90] It is evident that the nature of the self-assemblies of molecular amphiphiles varies significantly and is highly dependent on the molecular structures. In this respect, it is important to note that not only the type of amphiphile, but also the nature and position of the photoresponsive unit together with several other parameters (nature and number of non-covalent binding units, structural rigidity, geometrical change, change in polarity, etc.) will dictate the assembly and responsive function.

Photoresponsive molecular amphiphiles typically have been designed by the attachment of a photoresponsive unit either in the headgroup or incorporation at different positions in the hydrophobic chain (Figure 1b). A variety of photoresponsive molecules such as azobenzenes, stilbenes, dithienylethenes, spiropyrans, molecular motors, donor-acceptor Stenhouse adducts (DASAs) and photocleavable groups like nitrobenzyl or coumarins, are available to produce amphiphiles and can be used to control molecular self-assembled structures using light.^[91,92] The molecular structures and the related photoisomerization processes of the typical photoresponsive systems are shown in Scheme 1.



Scheme 1. Representative photoresponsive structures and their photoisomerization processes of (a) azobenzene, (b) stilbene, (c) dithienylethene, (d) spiropyran, (e) overcrowded alkene (molecular motor) and (f) donor-acceptor Stenhouse adducts (DASAs).

3. Dynamic functions of photoresponsive molecular amphiphiles in Gibbs Monolayers

When amphiphiles are introduced to aqueous media, the molecules spread over the entire interface with the hydro-

philic heads oriented towards the polar phase and the hydrophobic tails oriented towards the non-polar air phase, allowing for the formation of self-assembled monolayers at air–water interfaces. Depending on the solubility of the amphiphiles in aqueous media, the self-assembled monolayers are classified as Langmuir monolayers and Gibbs monolayers (adsorption monolayers).^[93–95] Langmuir monolayers, formed by insoluble or sparingly soluble amphiphiles, have attracted great interest due to the intrinsic properties facilitating the formation of well-organized layered films. Langmuir monolayers of photoresponsive amphiphiles containing azobenzene, spiropyran, stilbene, overcrowded alkene, and dithienylethene units, show controlled reversible surface pressure, and tightly packed thin films of assembled structures can be obtained by the Langmuir–Blodgett method, which indicates significant prospects for optical devices and sensing applications.^[96–115] Gibbs monolayers (adsorption monolayers), composed of water-soluble amphiphiles directly distributed at the air–water interfaces without the use of organic solvents, show tight correlations between assemblies in aqueous solution and at the air–water interface. In early studies of Gibbs monolayers of photoresponsive amphiphiles, some crucial equilibrium physical parameters, e.g., equilibrium surface tension and critical micelle concentration (CMC), were employed to reveal the self-assembly transformations at air–water interfaces and in solutions.^[116–125] In this section, we will focus on dynamic functions of photoresponsive molecular amphiphiles in Gibbs monolayers.

In 1999, Shin and Abbott^[126] reported the active control of dynamic surface tension of mixed surfactants containing sodium dodecyl sulfate (SDS) and a photoresponsive azobenzene bolaamphiphile **1** (Figure 2a). Positively charged

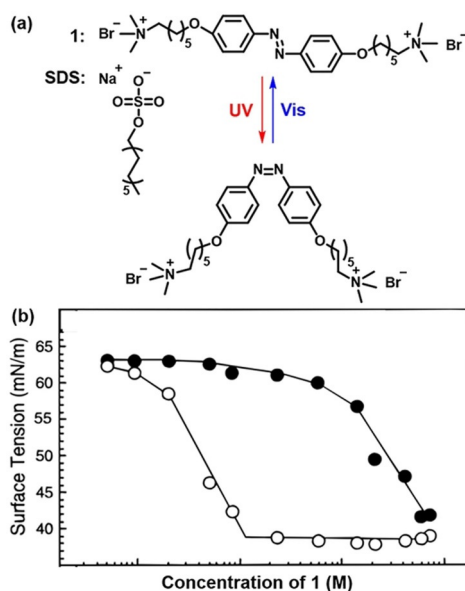
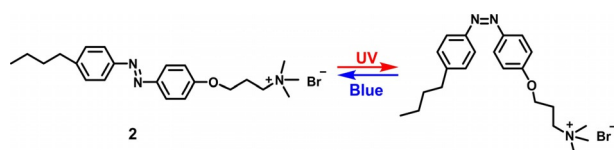


Figure 2. (a) Molecular structures and photoisomerization of **1** and SDS. (b) Dynamic surface tension of aqueous solutions of **1** with SDS (1.6 mM) before (filled circles) and after (open circles) UV light irradiation. The surface tension was measured by the du Noüy ring method.^[128] Adapted with permission from ref. [126]. Copyright 1999, American Chemical Society.

1 allows an intermolecular interaction with the negatively charged SDS. This complementary Coulombic interaction enables a closer packing of the co-assembled structure of both amphiphiles at the air–water interface, i.e., Gibbs monolayer. The geometrical transformation of azobenzenes upon irradiation, from *trans* to *cis*, induced a large change of dynamic surface tension up to 25 mN m^{-1} at a concentration of **1** below CMC (Figure 2b). This study demonstrated an elegant new principle for the dynamic control of surface tension of aqueous solutions, distinct from a change in surface tension at an equilibrium state, based on a photoresponsive amphiphile. It should be noted that the *trans*-*cis* isomerization in azobenzene systems not only affects geometry but a major change in dipole moment (typically around 3 D) also occurs. Later, Smith and co-workers found that the surface tension of a nonionic azobenzene amphiphile film showed a dependence on irradiation and age.^[127] On the basis of the dynamic surface tension data, they proposed a mechanism of competitive adsorption between the *trans* and *cis* isomers. The precise adsorption and self-assembly behavior of these azobenzene amphiphiles in the *trans* and *cis* geometries at the air–water interfaces, which induced the change of surface tension, are still to be elucidated.

Monteux and co-workers^[129] designed a photoresponsive amphiphile **2** comprising a cationic ammonium head group and an azobenzene-based hydrophobic tail (Scheme 2) to investigate dynamic adsorption/desorption behavior of **2** at the resulting photoresponsive air–water interface with tunable surface tension. Using a kinetically limited model taking into account the electrostatic barrier to adsorption, the authors found that *cis*-**2** adsorbed 10 times faster than *trans*-**2** isomer but desorbed 300 times faster, resulting in monolayers packed almost exclusively with *trans*-**2** under equilibrium conditions. Due to the competition between the *trans*- and *cis*-isomers, changes in surface assembly occurred in a few seconds, allowing to trigger rapid variations of interfacial properties. In order to observe the surface flux, a suspension containing **2** (1.15 mM) and talc particles was investigated by microscopy. When a UV light spot ($\lambda = 365 \text{ nm}$) was employed on the surface of the solution, a majority of *trans*-**2** was adsorbed outside the light spot, while *trans*-to-*cis* isomerization inside the light spot leads to desorption of **2** from the interface, resulting in a rapid increase of surface tension. This surface tension gradient resulted in a Marangoni flow from the outside to the inside of the light spot, which induced the movements of talc particles towards the light spot. Therefore, a particle concentrating behavior in the light spot was observed in a few seconds after exposure to UV light (Figure 3). Interestingly, such particle concentrating behavior not only can be induced by UV light but also by blue light ($\lambda = 436 \text{ nm}$). This study demonstrated a distinct difference of



Scheme 2. Molecular structures and photoisomerization of azobenzene amphiphile **2**.

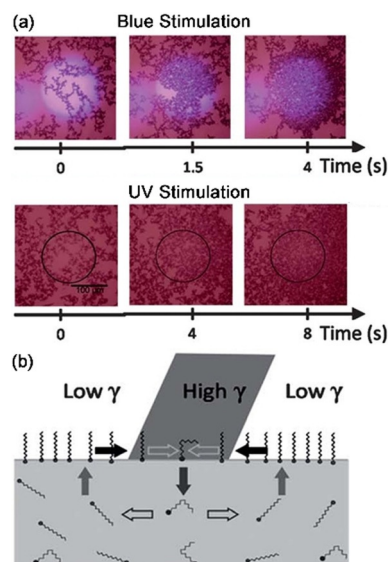


Figure 3. (a) Photograph of particle concentrating behavior under a UV or a blue light spot. (b) Schematic illustration of the photoresponsive amphiphile adsorption-desorption and the corresponding Marangoni flow. Adapted with permission from ref. [129]. Copyright 2011, Royal Society of Chemistry.

adsorption/desorption behavior of *trans*-**2** and *cis*-**2**, highlighting a new way to induce surface tension gradients at the air–water interface of an azobenzene amphiphile-containing solution and achieve light-induced Marangoni flow.

Taking advantage of the dynamic and tunable interfacial properties of aqueous solutions of azobenzene amphiphile **2**, Monteux's group also reported photoresponsive foams with in situ photo-controlled stability and breakage. These were prepared from aqueous solutions of **2**, providing a non-invasive method to remotely control the stability of foams (Figure 4a).^[130] Stable foams were obtained from aqueous

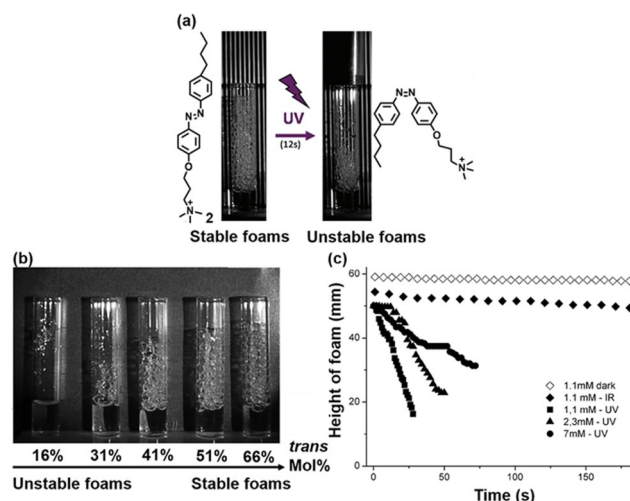


Figure 4. (a) Schematic illustration of photoresponsive foams prepared from a solution of **2**. (b) Stable foams are produced by *trans*-**2**. (c) Unstable foams are obtained by UV light irradiation. Adapted with permission from ref. [130]. Copyright 2012, American Chemical Society.

solutions of **2**, predominantly in the *trans* state, which ruptured in a short time by exposure to UV light (Figure 4b,c). Notably, after irradiating the solutions obtained from the disintegrated foams with blue light for several minutes, it was possible to prepare stable foams again, indicating a reversible control of foam formation by alternating UV and blue light irradiation. Upon UV light irradiation of the stable foams, *trans-2* converted into *cis-2*, which subsequently desorbed from the air–water interfaces to the bulk solutions, providing dynamic adsorption/desorption interfaces. The authors proposed that due to the dynamic adsorption/desorption behavior of **2**, an out-of-equilibrium surface tension gradient induced Marangoni flows, which might lead to the breakage of foams during UV light irradiation.

To establish a correlation between the light-induced flow and the foam destabilization mechanism, Monteux and co-workers investigated the dependence of light-induced flow of **2** and foam breakage both at a micrometer length-scale (thin-liquid films of bubbles) and at a millimeter length-scale (macroscopic foams).^[131] In thin-liquid films, a tunable velocity of Marangoni flow was obtained by controlling the photoisomerization of **2** at the air–water interfaces using variable UV light intensities. The results obtained from experiments with macroscopic foams showed that the light-induced flow can slow down the foam drainage at the early stage of UV light irradiation, while a rapid rupture of foams was subsequently observed. Next, the influence of illumination on disjoining pressures of thin liquid films in identical foam systems was investigated, suggesting that the UV-light-induced rupture of foams was due to a decrease of electrostatic repulsion in the thin foam film as well as the oscillation of the disjoining pressure isotherm.^[132] This systematic study of an amphiphile-based photoresponsive system at the air–water interface emphasizes the prospects for application in remote control (by light) of foam stability.

In an approach toward a dual-stimuli responsive amphiphile **3**, Jiang and co-workers slightly modified the azobenzene amphiphile **2** to incorporate a tertiary amine head group (Figure 5).^[133] The amphiphile **3** could be reversibly transformed between a hydrophobic tertiary amine and an amphiphilic ammonium bicarbonate by alternately purging a solution of **3** with N₂ and CO₂, respectively, which was confirmed by conductivity measurements. The *trans*-to-*cis*

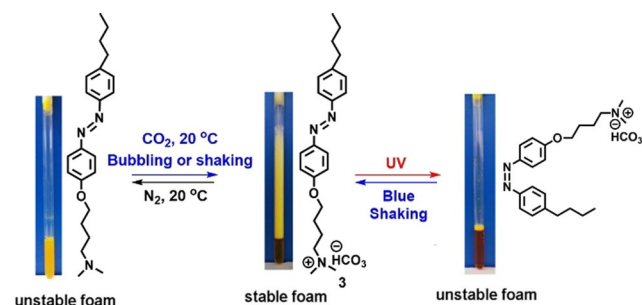


Figure 5. Schematic illustration of dual-stimuli responsive foams prepared from solutions of **3**. Adapted with permission from ref. [133]. Copyright 2017, ScienceDirect, Elsevier B.V.

photoisomerization of **3** induced by UV light ($\lambda = 365$ nm) afforded a *trans-3*/*cis-3* ratio of 4/96 at the photostationary state (PSS) and the back isomerization was induced by exposure to blue light. Due to the major structural and geometrical transformation of **3** triggered by both CO₂/N₂ and light, dual-stimuli responsive foams were obtained. Stable foams, prepared from *trans-3* solutions bubbled with CO₂, were ruptured in 10 min after purging with N₂. Alternatively, the disruption of stable foams could be induced by UV light irradiation, providing as a simple but promising strategy for the creation of multi-stimuli responsive systems (Figure 5).

Except for the previously discussed modifications of the hydrophilic moieties of azobenzene amphiphiles, an azobenzene amphiphile **4** with an anionic group as well as enhanced structural rigidity of its hydrophobic part was designed, which was anticipated to provide photoresponsive foams with more significant differences of foam stability before and after exposure to light (Figure 6).^[134] The photoisomerization of **4** was investigated by UV-vis and ¹H NMR spectroscopy and the amount of *cis-4* obtained after exposure to UV light was estimated to be 95% at the PSS. With a more rigid hydrophobic moiety, a drastic variation of CMC between *trans-4* and *cis-4* was observed, reflecting in a large geometrical transformation and difference in aggregation between these two isomers. Additionally, stable foams with a half-life of ≈ 16 h were obtained from a *trans-4* solution (2 mM), which were more stable than those prepared from other reported azobenzene amphiphiles. In sharp contrast, all the stable foams collapsed within 4 min after irradiation with UV light (isomerization to *cis-4*), providing photoresponsive foams with a dramatic variation of foam stability triggered by light.

The modification of the cationic azobenzene amphiphile **2** by replacing the bromide counterion by a bis-(trifluoromethanesulfonimide), [BTF] anion, provided a new strategy to control foam stability by reversible binding to cucurbit[7]uril (CB[7]) and spermine moieties (Figure 7).^[135] The foamability of azobenzene amphiphile **5**, containing an [Azo] tail and [BTF] anion, was significantly improved after the addition of CB[7], which was attributed to a closer packing of the [Azo] tails at the air–water interfaces. The formation of the host-guest complex of **5**⊂CB[7], as confirmed by ¹H NMR spectroscopy and conductivity measurements, might shield the electrostatic interaction between [Azo] and [BTF] to

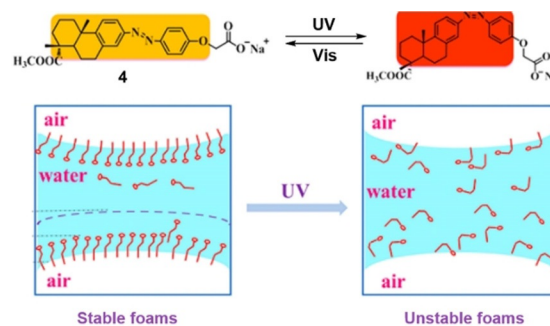


Figure 6. Schematic illustration of photoisomerization and photoresponsive foams prepared from a solution of **4**. Adapted with permission from ref. [134]. Copyright 2017, American Chemical Society.

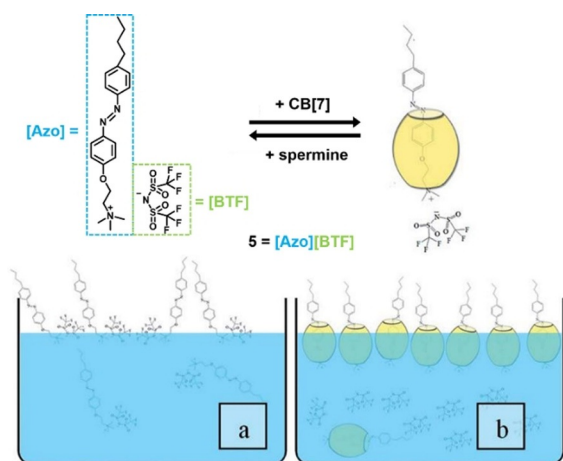


Figure 7. The proposed structural transformation at the air–water interface of aqueous solutions of (a) **5** and (b) complex of **5**⊂**CB[7]**. Adapted with permission from ref. [135]. Copyright 2016, Royal Society of Chemistry.

induce the desorption of **[BTF]** from the interfaces, which allows for the closer packing of the **[Azo]** tails. With the addition of spermine, a stronger host-guest interaction of spermine⊂**CB[7]**, compared to **5**⊂**CB[7]**, resulted in a removal of **CB[7]** from the complex of **5**⊂**CB[7]**, providing a switching back to a loose-packed monolayer of **5** at the air–water interface and a simultaneous decrease in the foamability. These results demonstrate an alternative strategy to reversibly control the foamability of the photoresponsive amphiphile by a supramolecular host-guest approach.

Aiming at industrial applications, Wang and co-workers synthesized a series of nonionic and cationic azobenzene amphiphiles by modifying the hydrophobic chain and the hydrophilic parts for the purpose of preparing photoresponsive foams for textile foam coloring systems to reduce pollutant discharges and energy consumptions of the traditional textile coloring process.^[136–141] The foamability and stability of the corresponding colored photoresponsive foams were reversibly tunable by light-stimuli. In this way, stable foams can be used in the textile coloring process with excellent performance, while the photo-controllable rupture of the stable residual foams enabled them to be readily recycled, allowing for a nearly zero-pollutant discharge coloring process (Figure 8).^[141] In addition to textile coloring, photoresponsive foams prepared from azobenzene amphiphiles are also employed in flotation processes of quartz particles.^[142,143] The results are promising for applications of photoresponsive molecular amphiphiles in more environmental-friendly industrial processes.

Dynamic photoresponsive air–water interfaces based on the isomerization of amphiphiles, also provide opportunities to control other macroscopic functions, such as liquid droplet motions,^[144,145] optical particle depositions with predefined patterns,^[146,147] and liquid marble transport.^[148] Similar to the particle concentrating behavior in the solution of amphiphile **2** by light-induced Marangoni flow,^[129] a strategy to accumulate particles at predefined positions with complex patterns was reported. Towards this goal, the light-induced Marangoni



Figure 8. Schematic illustration of a recycled foam coloring process based on photoresponsive foams. Adapted with permission from ref. [141]. Copyright 2019, ScienceDirect, Elsevier B.V.

flow in an evaporating droplet containing a cationic azobenzene amphiphile **6** was explored (as illustrated in Figure 9a).^[146] Using photomasks, a broad variety of complex patterns were obtained in arbitrary particle systems, ranging from model suspensions to complex “real-world” formulations such as commercial coffee suspensions. Meanwhile, a solution of amphiphile **6** was also employed to demonstrate a light-driven transport of floating liquid marbles based on

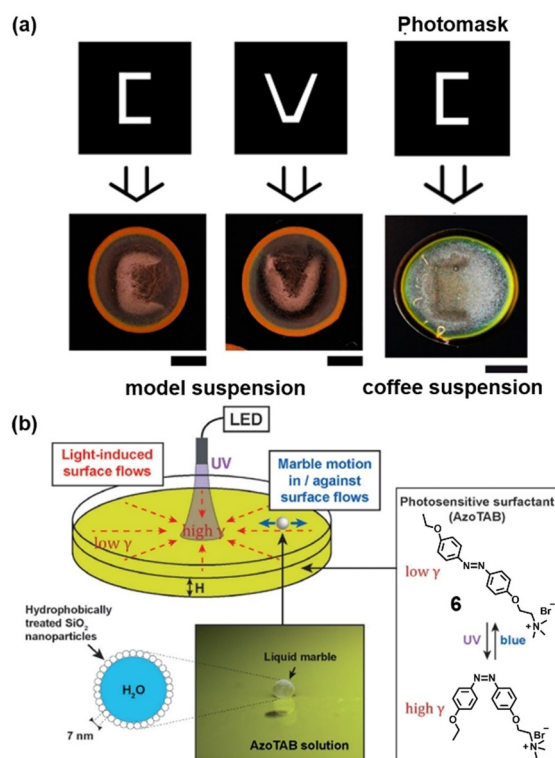


Figure 9. Schematic illustration of (a) optical particle depositions with predefined patterns and (b) light-driven transport of a floating liquid marble. Adapted with permission from ref. [146]. Copyright 2016, American Chemical Society. Adapted with permission from ref. [148]. Copyright 2016, Wiley-VCH.

Marangoni flow at the air–water interface (Figure 9b).^[148] Interestingly, two motion directions of the liquid marbles, including Marangoni motion (i.e., in the same direction of the Marangoni flow) and anti-Marangoni motion, were observed by controlling the thickness of the liquid substrate, showing a more complex dynamic function of photoresponsive amphiphiles at the air–water interface.

Recently, Baigl and co-workers have developed a novel photoresponsive dissipative self-assembling system by employing micromolar amounts of **6** (Figure 9) in a suspension of anionic polystyrene microparticles. The particle organization can be reversibly and dynamically actuated between a highly crystalline assembly (under UV or blue light irradiation) and a disordered state (in the dark) with a fast response time at the air–water interfaces (Figure 10).^[149] The controllable crystallization and disassembly processes of the particles were driven by the light-induced dynamic adsorption/desorption behavior of **6** at the air–water interface. In the absence of light, the suspension was composed of pure *trans*-**6**, and the particles formed disordered structures. After irradiating for 1 min, the suspension at the PSS was composed of 95 % of *cis*-**6** (UV-light) or 45 % of *cis*-**6** (blue-light). Although the PSS obtained by UV light or blue light irradiation were significantly different, the response of the colloidal assembly at the air–water interface was strikingly similar, i.e., the formation of highly crystalline colloidal assemblies after ≈ 10 s, indicating that the crystallization and the disassembly were not controlled by the bulk composition of **6**. The authors proposed that the continuous light-induced desorption of **6** maintained the system out-of-equilibrium and allowed the crystallization process to occur. When the light was switched off, the crystals were transferred to the disordered phase. This was the first report of a photoresponsive amphiphile allowing controlled transformations of a colloidal assembly at the air–water interface, expanding the realm of currently known dissipative systems.

Ravoo, Braunschweig, and co-workers introduced azo-derived photoresponsive amphiphiles **7** and **8** (Figure 11), and investigated their responsive adsorption property, mainly

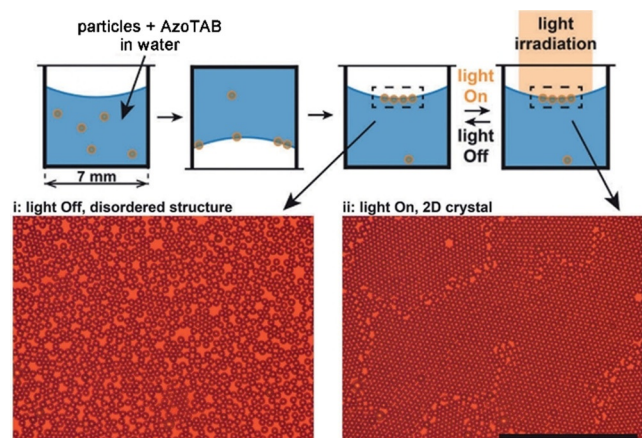


Figure 10. Transmission microscopy images of light-induced (i) disassembly and (ii) colloidal crystallization at the air–water interfaces. Scale bar: 100 nm. Adapted with permission from ref. [149]. Copyright 2019, Wiley-VCH.

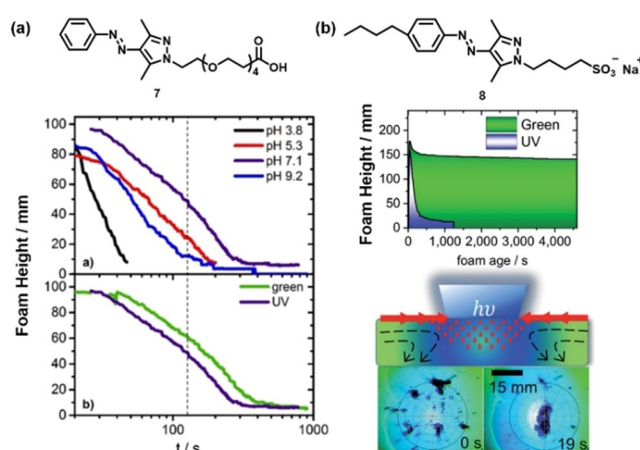


Figure 11. (a) Photo- and pH-responsive foams prepared from solutions of **7**. (b) Photoresponsive foams and light-actuated particle motion prepared from solutions of **8**. Adapted with permission from ref. [150]. Copyright 2018, American Chemical Society. Adapted with permission from ref. [151]. Copyright 2020, Royal Society of Chemistry.

using vibrational sum-frequency generation (SFG) and dynamic surface tension measurement, as well as their corresponding macroscopic functions, e.g., responsive foams and particle motions. The surface tension and foam stability of aqueous solutions of **7**, featuring a carboxylate end-group connected with ethylene glycol linker, showed dependence on external stimuli such as pH and light (Figure 11a).^[150] At various pH conditions of solution **7**, the highest foam stability was observed at pH 7.1 after green light irradiation. Furthermore, amphiphile **8**, with a sulfonate end-group connected by an alkyl linker, can attain higher foam stability than that observed with **7**, possibly due to the improved micro-phase separation by the hydrophobic alkyl-chain (Figure 11b).^[151] This study clearly demonstrates an alternative class of photoresponsive amphiphiles suitable to control foam stability and light-actuated particle motions by modulating the dynamic absorption and desorption properties of Gibbs monolayers.

In addition to the azobenzene and azo-derived amphiphiles, spiropyran-based amphiphiles also can form dynamic photoresponsive Gibbs monolayers to allow applications in responsive foams and induce controlled motion.^[152–154] Light- and pH-responsive foams were obtained from solutions of amphiphile **9** (Figure 12).^[154] Additionally, it is noted that a color change (yellow to dark red) of amphiphile **9** can be finely adjusted by pH (2.1 to 10.5). Meanwhile, in the pH range of 4.8 to 5.9, a reversible color change of amphiphile **9** between orange and yellow was observed by alternating exposure to light or no illumination. Taking advantages of the photoresponsive color properties, photo-writing of information and subsequent self-erasing can be achieved upon irradiation with a photomask on top of the aqueous solution of **9**.

Single head/single tail photoresponsive ionic molecular amphiphiles with a short hydrophobic chain have been mainly used to control dynamic interfacial properties effectively at Gibbs monolayers by the transformation of molecular configuration. This is possibly due to their good solubility,

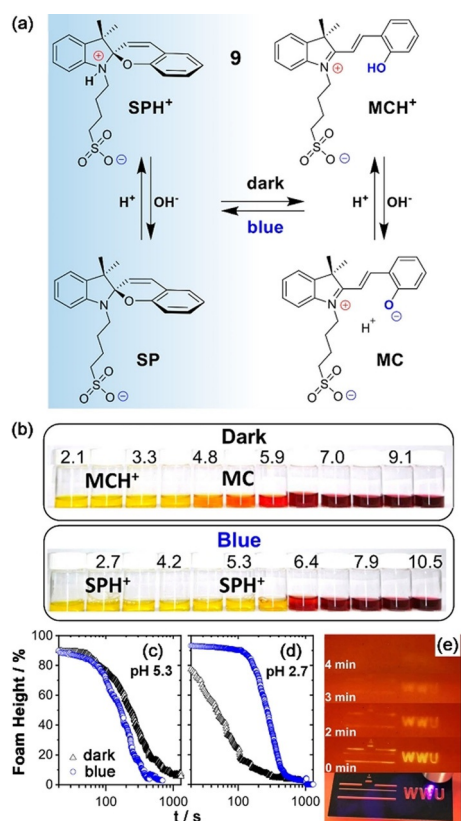


Figure 12. Schematic illustration of (a) isomerization processes of amphiphile **9** and (b) photo- and pH-responsive color change in solutions. Photoresponsive foams prepared from the solution of **9** at pH (c) 5.3 and (d) 2.7. (e) Photo-writing of information and self-erasing functions in a solution of **9** (pH 5.3) upon 405 nm light irradiation with a photomask. Adapted with permission from ref. [154]. Copyright 2020, American Chemical Society.

intrinsic fast absorption at air–water interface as well as simple molecular design and synthesis.^[155,156] In addition to the destabilization of Gibbs monolayers using photocontrolled alteration of molecular configuration, the formation of a zwitterionic state of a spiropyran amphiphile might be serving as an alternative strategy to control interfacial properties at Gibbs monolayers.^[154] It is evident from the responsive systems discussed here that the control of macroscopic function based on aqueous soluble photoresponsive amphiphiles (below 1.0 wt %) assembled as Gibbs monolayers offers numerous attractive opportunities for developing environmental-friendly (industrial) processing techniques. However, to identify the mechanisms of assembly and amplification along length scales from molecular photoisomerization at air–water interfaces to macroscopic functions, such as macroscopic photoresponsive foams and particle motion and collection, remains highly challenging. Our group recently reported unique dynamic assembly transformations of a novel molecular motor amphiphile both at the air–water interface and in solution, allowing for multiple-states switching of macroscopic foams, controlled by light/heat stimuli. This shed light onto the mechanism of amplification, from multiple reversible photochemical and thermal isomerization processes at the molecular level, to various dynamic assem-

blies at the microscopic scale and responsive foam properties at the macroscopic level (a detailed discussion is provided in Section 4.1).^[157] However, the use of amphiphiles containing other photoresponsive units employed at air–water interfaces, as well as the application of photoresponsive molecular amphiphiles in developing more environmental-friendly processes in industry instead of laboratory demonstrations remain largely unexplored.




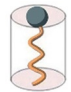
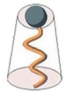

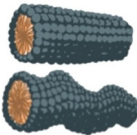

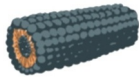
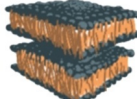
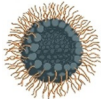
4. Functional supramolecular self-assembly of photoresponsive molecular amphiphiles in solution

The self-aggregation of amphiphilic molecules has long been known to yield a rich variety of assembled structures, including micelles (spherical, rod-like, and worm-like) and bilayers structures (vesicles, tubules, and planar lamellae), in organic, aqueous, or mixed organic–aqueous media. Since the supramolecular self-assembled structures of amphiphiles in aqueous media allow compatibility to natural systems as well as the potential for biologically relevant applications, we focus on the self-assembled microstructures and the structural transformations of molecular amphiphiles in aqueous media. The observed assemblies depend on the molecular structures and experimental conditions, such as concentration, temperature, pH, light, ionic strength, and the structure of the co-assembly compound.^[81,158–165] According to Israelachvili et al.,^[6] the shape and size of self-assembled structures of amphiphiles in aqueous media can be predicted by using the packing parameter, P . The packing parameter was defined as: $P = v/a_0l_0$, where v is the volume of the amphiphile tail, a_0 and l_0 are the area of the hydrophilic groups and the length of tail in the amphiphile, respectively. Therefore, a geometrical change of amphiphiles would affect the packing parameter P , and in response result in transformations of self-assembled structures (Table 1.1).^[6,16,158,166] In this section, we focus on the self-assembled structures of photoresponsive amphiphiles in aqueous media, ranging from one-dimensional (1D) nanostructures, isotropic entangled three-dimensional (3D) networks to anisotropic 3D structures.

4.1. Isotropic self-assembly of photoresponsive molecular amphiphiles

Self-assembly of photoresponsive molecular amphiphiles into one-dimensional nanostructures offers insight into how to achieve precise control over supramolecular organization and many opportunities for applications in biological systems, e.g., tissue regenerative supramolecular scaffolds. In the context of biomaterials and supramolecular chirality, a single-handed helical structure has always been an attractive target.^[167–173] The Stupp group reported a transformation of a photoresponsive peptide amphiphile **10a** from a quadruple helical fiber into single fibers in aqueous media (Figure 13).^[174] Using a photodeprotection strategy, the peptide amphiphile **10a** was designed to contain a palmitoyl tail, a 2-nitrobenzyl protecting group, and an oligopeptide

Table 1: Different self-assembled structures predicted by the packing parameter P .

P value	$P \leq 1/3$	$1/3 < P \leq 1/2$	$1/2 < P < 1$	$P = 1$	$P > 1$	
Structure of amphiphiles						
Aggregates	Spherical micelles	Rod-like or worm-like micelles	Vesicles	Tubules	Lamellae	Reversed micelles
Model of aggregates						

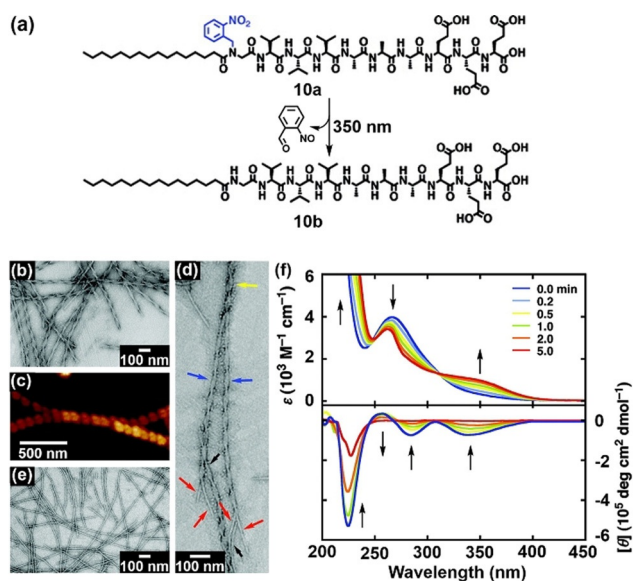


Figure 13. Schematic illustration of the photocleavage process from **10a** to **10b** upon irradiation. (b) TEM and (c) AFM images of **10a** in aqueous media (pH 11). (d) TEM image of a quadruple fiber: the quadruple strand (yellow arrow) uncoils into double helices (blue arrows) and further into single fibers (red arrows). (e) TEM image of a solution of **10a** after irradiation. (f) UV-vis (top) and CD (bottom) spectral changes of **10a** in aqueous media upon irradiation. Adapted with permission from ref. [174]. Copyright 2008, American Chemical Society.

segment $GV_3A_3E_3$ (Gly-Val-Val-Val-Ala-Ala-Ala-Glu-Glu-Glu), in which the 2-nitrobenzyl group can be cleaved by irradiation at 350 nm to afford **10b** (Figure 13a). Due to the unfavorable hydrogen bond formation attributed to the steric hindrance of the 2-nitrobenzyl group, different supramolecular architectures of **10a** and **10b** were observed by transmission electron microscopy (TEM). TEM and atomic force microscopy (AFM) images of **10a** revealed rare quadruple helix assemblies with a nearly uniform width and helical pitch of 33 ± 2 and 92 ± 4 nm, respectively (Figure 13b–d). After the photocleavage of the 2-nitrobenzyl group by 350 nm light irradiation for 5 min, the UV-vis and circular dichroism (CD) spectra (Figure 13f) and the TEM image (Figure 13e) revealed the dissociation of the quadruple helix assemblies into single non-helical fibrils based on the non-switchable photodeprotection strategy. This study suggests novel strat-

egies to create functional and photoresponsive helical supramolecular architectures with prospects for sensing or actuation.

Subsequently, Stupp and co-workers replaced the oligopeptide segment $GV_3A_3E_3$ of **10a** by a fibronectin epitope Arg-Gly-Asp-Ser, providing a new photoresponsive peptide amphiphile **11a** (Figure 14a).^[175] According to Hargerink et al.,^[176] the modification of molecular sequences in the β -sheet domains will affect the resulting assembled structures. Indeed, due to a weaker β -sheet-forming sequence of **11a** (compared to **10a**), a clear solution remains under the self-assembling conditions (4.0×10^{-4} M in 0.1 M $CaCl_2$ aqueous solution, Figure 14b), while using identical conditions, the quadruple-helix-forming **10a** generated nanofibers and gels. However, **11b**, obtained by irradiation of **11a** with 350 nm

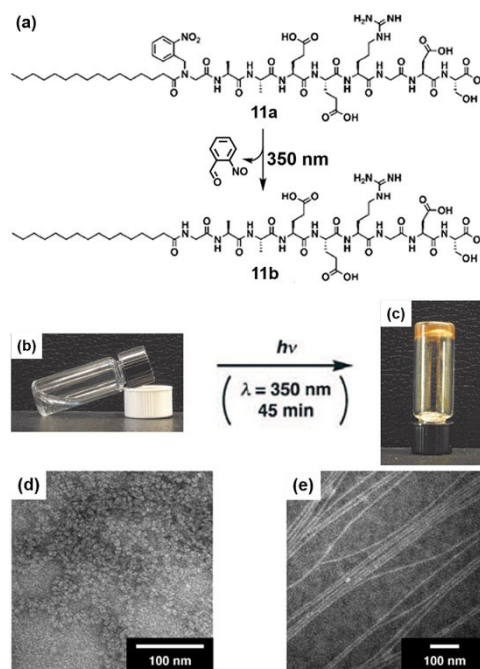


Figure 14. Schematic illustration of (a) the photocleavage process from **11a** to **11b** and a sol-to-gel transformation of **11a** in $CaCl_2$ solution (b) before and (c) after 350 nm light irradiation. TEM images of structures formed by deposition of **11a** in $CaCl_2$ solution (d) before and (e) after irradiation. Adapted with permission from ref. [175]. Copyright 2009, Wiley-VCH.

light, generated a transparent gel, demonstrating a 3D sol-to-gel transition in response to light (Figure 14c). The TEM images of **11a** and **11b** revealed a transformation from nanospheres (12 ± 2 nm in diameter) in **11a** to nanofibers (11 ± 1 nm in diameter) in **11b** (Figure 14d,e). Furthermore, both **11a** and **11b** showed no cytotoxicity, meanwhile, the light-triggered gelation of **11a** increased its bioactivity, allowing photoresponsive cell scaffold development.

Except for supramolecular architectures with multiple helices, the design of other dynamic, but well-defined complex architectures with adaptive behavior in response to external stimuli is one of the challenges towards artificial nanostructures. A photoresponsive self-assembled vesicle-capped nanotube system in water of amphiphile **12**, containing an overcrowded alkene core, was firstly developed by our group (Figure 15a).^[177] In the presence of common phospholipid, 1,2-dioleoyl-*sn*-glycero-3-phosphocholine (DOPC), unique vesicle-capped nanotube self-assembled structures were observed by cryogenic transmission electron microscopy (cryo-TEM). The nanotubes are exceptionally stable in water as the capping vesicle can be chemically altered or removed and reattached by adding/removing Triton X-100, without affecting the nanotubes (Figure 15c). Alternatively, the vesicle-capped nanotubes can be selectively disassembled by photochemical conversion in an irreversible process (Figure 15b). The fluorescent nature of the overcrowded alkene

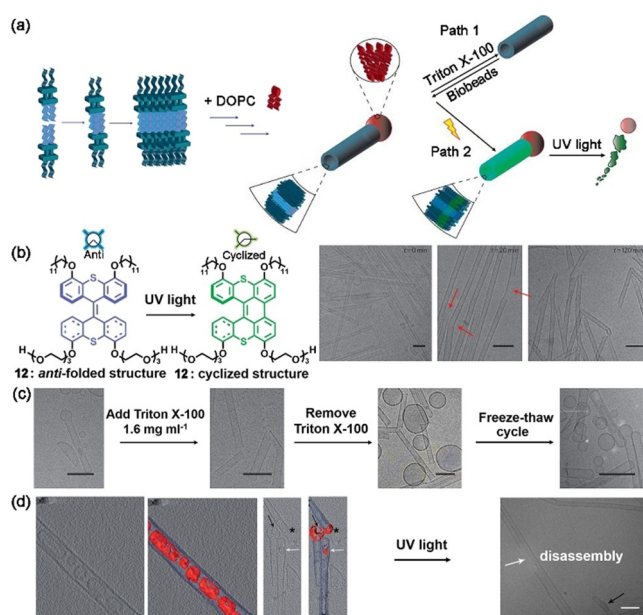


Figure 15. (a) Schematic illustration of controllable structural transformation of co-assemblies of amphiphile **12** and DOPC. (b) Transformation of amphiphile **12** and Cryo-TEM images of the photo-induced disassembly process. Cryo-TEM images were taken at $t = 0$ min, 20 min, and 120 min. (c) Cryo-TEM images of the reversible assembly and disassembly of vesicle controlled by Triton X-100. (d) Cryo-TEM images of osmosis-induced nanotubes encapsulated vesicles and photo-induced disassembly of nanotubes. Scale bars in (b,c) = 100 nm, in (d) = 50 nm. Adapted with permission from ref. [177]. Copyright 2011, Macmillan Publishers Limited, part of Springer Nature. Adapted with permission from ref. [178]. Copyright 2015, Wiley-VCH.

core allowed the observation of self-assembly transformations in real time using fluorescence microscopy. The reversible vesicle removal and light-induced disassembly processes of the vesicle-capped nanotube provided a strategy to trigger and control supramolecular self-assembly architectures in a complex multi-component system by using a combination of chemical composition and light-stimuli. The vesicle from the vesicle-capped nanotube, was also shown to be sensitive to osmotic pressure, allowing the vesicles to be encapsulated into the nanotube while subsequent disassembly of the nanotube and release of the vesicles could be induced upon irradiation (Figure 15d).^[178] This strategy clearly demonstrates the multiple responsiveness and complex behavior of these novel co-assembling systems.

UV light is widely used in most of the light-stimulated systems. However, the low penetration and damaging nature of UV light in biosystems limit in vivo applicability of UV-sensitive materials. In this regard, photoresponsive systems, triggered by near-infrared light (NIR) at longer wavelengths with lower cytotoxicity and deeper penetrating depth, provide a promising solution for future in vivo applicability. Recently, Wang's group used coumarin to modify lipid molecules as the basis for a photoresponsive lipid amphiphile, enabling the preparation of NIR-responsive liposomes for potential drug delivery,^[179] although the self-assembly transformation of the obtained liposomes was not studied in depth. Toward this goal, a new UV/NIR responsive amphiphile **13a**, which co-assembled with a common surfactant, tetradecyldimethylamine oxide (C₁₄DMAO), was introduced as the basis for a dual-responsive self-assembly system (Figure 16).^[180] Depending on the concentration of **13a**, the formation of worm-like micelles (30 mM) or vesicles (50 mM) in C₁₄DMAO solutions was observed. Although the reason for the NIR responsiveness remains unclear, both the worm-like micelles and vesicles can be transformed into spherical micelles triggered by NIR light irradiation because of the photocleavage of **13a**.

The aforementioned systems, while based on irreversible photoresponsive amphiphiles, showed the potential of controllable supramolecular self-assembled structures in aqueous media ranging from one-dimensional nanostructures transformations to isotropic entangled three-dimensional sol-gel transformations. However, reversible transformations of self-assembled structures could provide more interesting and sophisticated opportunities toward the development of smart materials. In early research on self-assembled structures of photoresponsive molecular amphiphiles, the Engberts group reported a series of investigations on the co-assembly behavior and molecular interactions in aqueous solutions of common surfactants and azobenzene amphiphiles (on the basis of azo dyes, e.g., methyl orange and ethyl orange), providing vital information for future fundamental and systematic study of molecular amphiphilic co-assembly systems.^[181–184] Recently, reversible photoresponsive molecular amphiphiles have been employed to control nanostructure transformations in solution. For instance, the Stupp group reported supramolecular helical nanofibers with a reversibly tunable pitch, formed by a photoresponsive peptide amphiphile **14** containing an azobenzene group (Figure 17a).^[185] A

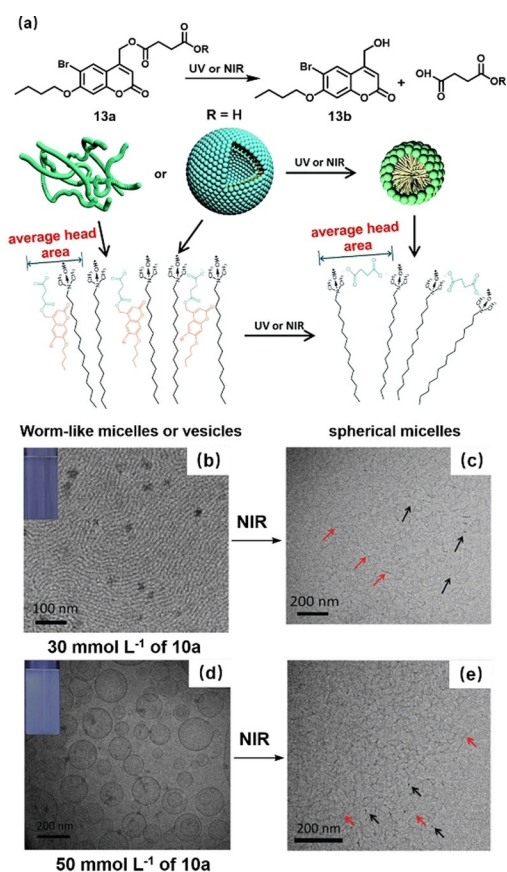


Figure 16. (a) Schematic illustration of the photocleavage process from **13a** to **13b** and the corresponding assembly transformations. Cryo-TEM images of solutions containing **13a** (30 mM) and C₁₄DMAO (b) before and (c) after NIR light ($\lambda = 808$ nm) irradiation inducing transformations from worm-like micelles to spherical micelles. Cryo-TEM images of solutions containing **13a** (50 mM) and C₁₄DMAO (d) before and (e) after NIR light irradiation inducing transformations from vesicles to spherical micelles. Adapted with permission from ref. [180]. Copyright 2017, Royal Society of Chemistry.

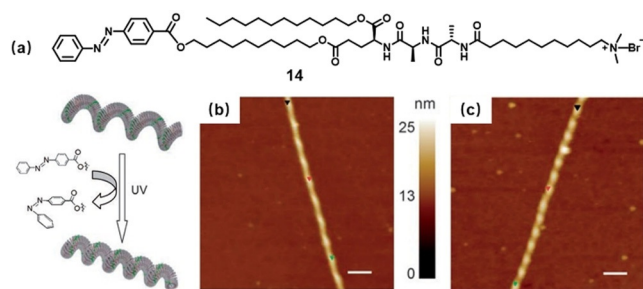


Figure 17. (a) Molecular structure of photoresponsive peptide amphiphile **14**. AFM images demonstrating reversible control of helix pitch of nanofibers (b) before and (c) after UV light irradiation. Adapted with permission from ref. [185]. Copyright 2007, Wiley-VCH.

suspension of nanofibers of **14** was irradiated with 360 nm light to induce photoisomerization from *trans*-**14** to *cis*-**14**. It was reasoned that the *cis* isomer is less planar than the *trans* isomers and consequently, the isomerization should increase the sterically-induced torque, leading to a reduction of the

helical pitch. Indeed the helix pitch of the nanofibers formed by *trans*-**14** decreased from 78 ± 4 nm to 56 ± 4 nm upon 365 nm light irradiation, as shown by the AFM images (Figure 17b,c). However, the self-assembly of **14** occurred in the presence of organic solvents, which limited the biocompatibility of this system.

Azobenzene-based photoresponsive amphiphiles are widely investigated regarding their assembling transformations in aqueous media, including cationic, bola-form, gemini, and nonionic type, which are co-assembled with common amphiphiles, e.g., SDS.^[186–195] Showing structural transformations from vesicles to other forms of assembled structures upon photoirradiation, e.g., nanofibers, these systems have potentials for applications in drug encapsulation and delivery.^[18, 65, 196, 197] In the aforementioned systems, the assemblies of azobenzene amphiphiles mainly transform between two states. The development of photoswitching assemblies in aqueous media as well as control of molecular self-assembly along multiple length-scales remain highly challenging. Huang and co-workers reported photoresponsive nanostructures with multi-states by a co-assembly of an azobenzene amphiphile **15** and a common amphiphile, cetyltrimethylammonium bromide (CTAB, Figure 18).^[198] The co-assembly structures of **15** and CTAB exhibit reversible transformations from worm-like micelles, vesicles, and lamellar structures to small micelles in aqueous solutions controlled by the irradiation time. Based on the photoisomerization of **15**, the distinct changes of molecular self-assembly structures were achieved, resulting in significant changes in macroscopic properties. According to the rheology behavior of the solution of **15** and CTAB, i.e., a transformation from a transparent, gel-like solution to biphasic solution, and homogenous solution upon prolonging 365 nm light irradiation, the co-assembly structures have been classified into four states: (1) worm-like micelle (89% of *trans*-**15**), (2) bilayer vesicle and planar lamellae (68% of *trans*-**15**), (3) worm-like micelle (37% of *trans*-**15**), and (4) micelle (17% of *trans*-**15**). Unfortunately, systematic structural analyses, e.g., cryo-TEM images, to confirm the self-assembled structures of these four states, were not provided. The same azobenzene

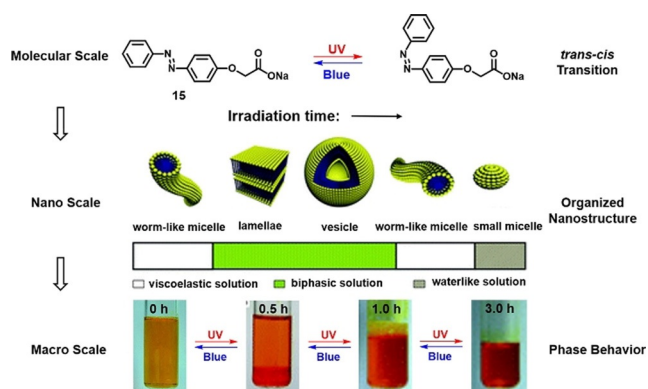


Figure 18. Schematic illustration of photo-controlled self-assembled systems with multi-states at multiple length-scales. Adapted with permission from ref. [198]. Copyright 2010, Royal Society of Chemistry.

amphiphile **15** was also co-assembled with a surface active ionic liquid.^[199] The co-assembly structures of worm-like micelles became slightly longer and more entangled (as shown by cryo-TEM) after 365 nm light irradiation, allowing to form a solution with a higher viscosity. However, no significant transformation of their self-assembled system was observed in studies by Yu et al.^[199] Self-assembly systems based on ionic liquids have attracted increasing attention due to their extraordinary properties, such as negligible vapor pressure, low melting point, and thermal stability.^[200,201] Recently, by introducing photoresponsive units into an ionic liquid, e.g., stilbene, cinnamate, and azobenzene, a series of novel photoresponsive ionic liquid have been designed,^[202–205] allowing for photocontrolled assembly transformations without co-assembly with other compounds.^[206–209] It is noted that the photoresponsive surface active ionic liquid with azobenzene in the headgroup, i.e., amphiphile **16**, showed dual-stimuli responsive and reversible transformations from vesicles to spherical micelles (Figure 19a).^[208] The photoisomerization of **16** was investigated by ¹H NMR and UV-vis spectroscopy, demonstrating a *trans*-**16**/*cis*-**16** ratio of 39/61 at the PSS after UV light irradiation for 30 min. A reversible transformation from vesicles (50 to 500 nm in diameter) to spherical micelles triggered by UV and visible light irradiation was observed in cryo-TEM images of the solution of *trans*-**16** (0.15 mM, Figure 19c–e), as predicted by DFT calculations. Furthermore, a transformation from vesicles to spherical micelles was also observed when the concentration of *trans*-**16** decreased from 0.15 mM (Figure 19c) to 0.05 mM (Figure 19b), demonstrating a concentration effect on the self-assembled structures. This study provided a means to achieve controlled self-assembly of distinct aggregates from a single component, i.e., a photoresponsive surface active ionic liquid.

Considering the systems discussed so far, photoresponsive self-assembly transformations were observed at the equilibrium state after the isomerization of amphiphiles. To provide a systematic understanding of the in situ self-assembly transformation, photoresponsive glucose-based amphiphilic micelles were monitored by using time-resolved small-angle neutron scattering (TR-SANS), as reported by the Wilkinson

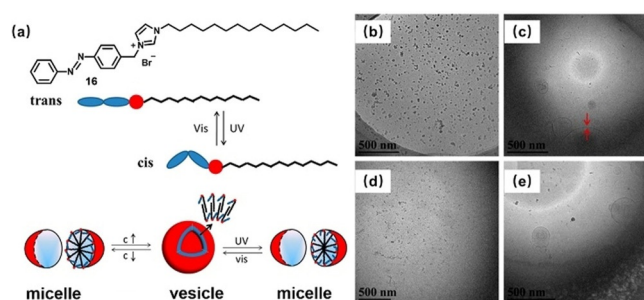


Figure 19. (a) Schematic illustration of molecular structure of **16** and proposed packing structures upon self-assembly of **16** in water. Cryo-TEM images of aq. solutions of **16** at a concentration of (b) 0.05 mM (micelle) or (c) 0.15 mM (vesicle) before UV light irradiation, (d) the solution of **16** (0.15 mM) irradiated with UV light (micelle) was (e) subsequently exposed to visible light (vesicle). Adapted with permission from ref. [208]. Copyright 2016, American Chemical Society.

group for the first time, to follow the evolution of the precise shape and aggregation number of micelles not only at the *trans*- and *cis*-states, but also at discrete time intervals.^[210] The *trans*-state of a glucose-based amphiphile assembled into micelles with aggregation number of about 290, and transformed to aggregation number of about 110, indicating that the size of the micellar structure was reduced upon UV light irradiation.^[211] Simultaneous usage of SANS and absorption spectroscopy can allow in situ monitoring of an azobenzene amphiphile transformation from worm-like micelles (*trans*-state) to fractal aggregates (at the PSS upon UV-light irradiation). Additionally, time-resolved small-angle X-ray scattering (TR-SAXS) was employed to follow the photo-induced disassembling process of an azobenzene-based amphiphile.^[212] All these measurements allow direct and in situ monitoring of the assembling transformations of photo-responsive amphiphiles to provide deeper insight into their transformation mechanism.

In addition to these distinct assembling structural transformation studies, a photoresponsive macroscopic gel-sol transformation of a gemini azobenzene-based amphiphile was reported by Zhao et al.^[213] Subsequently, Jiang and co-workers developed a dual stimuli-responsive entangled network, showing a three-dimensional sol-gel transformation formed by a co-assembly of a cationic azobenzene amphiphile **17** and a commercially available organic salt, sodium azophenol (**AzoONa**), as shown in Figure 20.^[214] The reversible structural transformation between **AzoONa** and **AzoOH** could be controlled through alternately purging with CO₂ and N₂ (studied by ¹H NMR). As a result, a gel-to-sol transformation was observed. Furthermore, this gel-to-sol transformation can also be induced by photoisomerization of amphiphile **17**. The dual stimuli-responsive gel-to-sol transformation was anticipated to have potential applications in microfluidics and tertiary oil recovery.

Molecular amphiphiles containing other photoresponsive units, such as diarylethenes, molecular motors, and spiropyrans, have been employed in the development of photo-responsive self-assembly systems. Illustrative (Figure 21 a) is

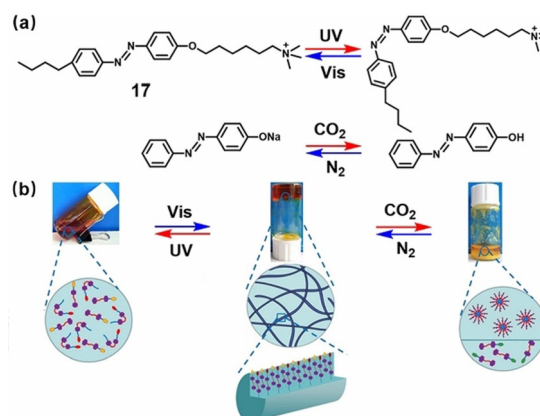


Figure 20. Schematic illustration of (a) photoisomerization processes of **17** and **AzoONa** and (b) a dual stimuli-responsive entangled three-dimensional sol-gel transformation. Adapted with permission from ref. [214]. Copyright 2018, ScienceDirect, Elsevier B.V.

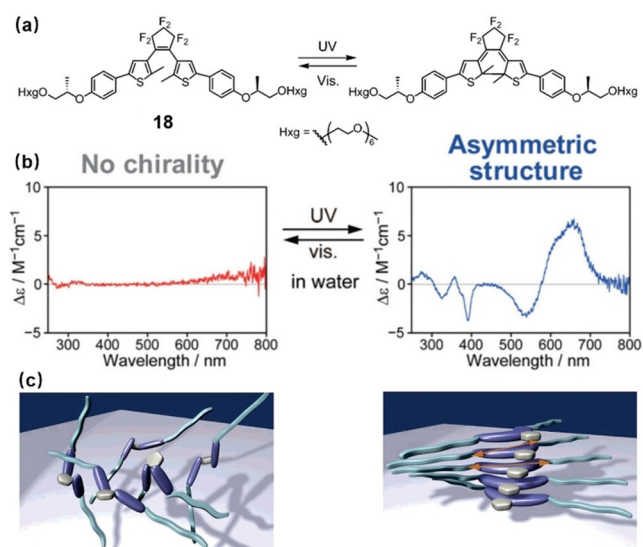


Figure 21. (a) Schematic illustration of photoisomerization processes of diarylethene-based amphiphile **18** containing hexa(ethylene glycol) (Hxg) side chains and stereogenic centres. (b) CD spectral change of **18** upon irradiation in an aqueous solution demonstrating that only the structure composed of the closed-**18** isomer exhibited supramolecular helicity. (c) Schematic illustration of the self-assembled nanostructure of (left) open-**18** and (right) closed-**18** in aqueous media. Adapted with permission from ref. [215]. Copyright 2006, American Chemical Society.

a chiral diarylethene-based amphiphile **18** containing hexa(ethylene glycol) (Hxg) side chains introduced by Irie.^[215] This photoresponsive amphiphile allowing for a light-dependent chirality transfer depending on the open-**18** and the closed-**18** isomers in aqueous solution (Figure 21b). The CD spectral data indicated that the assembled nanostructures of open-**18** do not induce supramolecular chirality while photogenerated closed-**18** induced supramolecular helicity (Figure 21c). The supramolecular helicity transformation between the open-**18** and the closed-**18** isomers might enable a new strategy for photoswitching chiroptical properties in aqueous media.

On the basis of our earlier reported amphiphile **12**, we designed a novel photoresponsive amphiphile **19** containing a molecular rotary motor core, in order to develop a multi-stage system for reversible self-assembly in water (Figure 22a).^[216] The photoisomerization and thermal helix inversion (THI) of amphiphile **19** were studied by UV-vis and NMR spectroscopy, which showed a metastable-**19**/stable-**19** ratio of 95/5 at the PSS with a half-life for the THI step of 270 h at 20 °C and 4.3 h at 50 °C. Tubular structures (Figure 22b), co-assembled by the motor amphiphile **19** and DOPC, were observed by cryo-TEM, which disappeared completely after 365 nm light irradiation for 15 min, and only bilayered vesicles were observed (Figure 22c). UV-vis and NMR studies indicated the formation of metastable-**19**, confirming that the isomerization of the motor amphiphile **19** induced the morphological transformations of the self-assembled structures. The sample, irradiated with 365 nm light for 15 min and subsequently heated at 50 °C for 16 h, showed multilamellar vesicles (Figure 22d). Tubular structures were observed again when the heated sample was

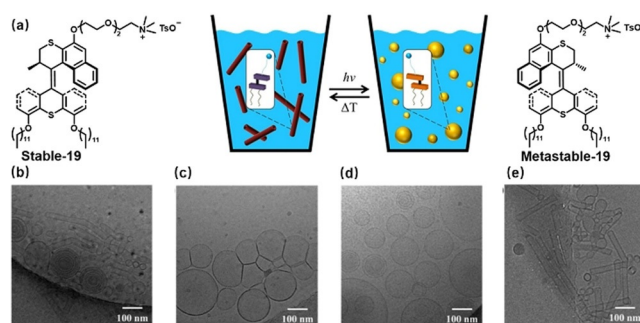


Figure 22. (a) Schematic illustration of isomerization processes of motor amphiphile **19** and the corresponding reversible self-assembly transformations between nanotubes and vesicles in aqueous media. Cryo-TEM images of co-assembled structures of stable-**19** and DOPC: (b) before and (c) after irradiation, (d) upon a subsequent heating process, and (e) freeze-thawing for 3 times after heating. Adapted with permission from ref. [216]. Copyright 2016, American Chemical Society.

exposed to a freeze-thawing process (Figure 22e), demonstrating a reversible self-assembly transformation between well-defined nanotubes and vesicles induced by light and heat. This was the first example, using a molecular motor amphiphile, which showed a reversible self-assembly transformation in aqueous media, providing a new generation of water-soluble photoresponsive amphiphiles, i.e., with a molecular motor core paving the way to increasingly complex and highly dynamic artificial nanosystems in aqueous media.

Recently, Kudernac and co-workers reported a visible light sensitive photoresponsive amphiphile **20**, composed of a spiropyran core, and demonstrated a reversible light-induced expansion of vesicles (Figure 23).^[217] The photoresponsive amphiphile **20** comprised an oligoether dendron as the hydrophilic moiety and a bent aromatic unit containing two spiropyran moieties as the hydrophobic moiety (Figure 23a). In an acidic aqueous solution of photoresponsive amphiphile **20**, the switching unit adopts the open protonated

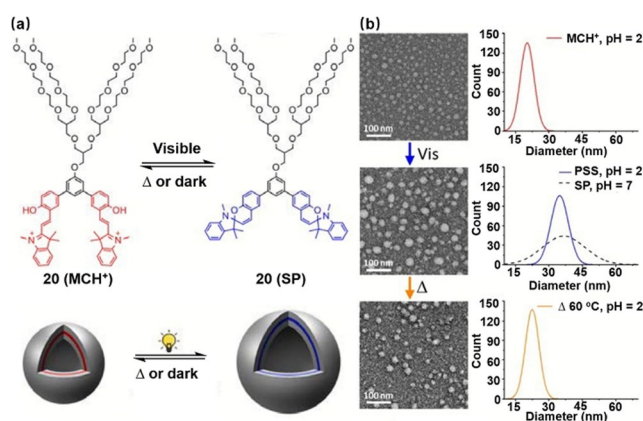


Figure 23. Schematic illustration of (a) isomerization processes of spiropyran-based amphiphile **20** and the corresponding reversible expansion of vesicles in water. (b) Light-induced reversible expansions from **20**(MCH⁺)-vesicles to **20**(SP)-vesicle in water (pH 2) determining by related size distributions in TEM images. Adapted with permission from ref. [217]. Copyright 2018, Royal Society of Chemistry.

merocyanine form (MCH^+). This MCH^+ form can be transiently converted into a closed and neutral spiropyran form (SP) by irradiation with visible light (Figure 23a). TEM images showed that both the $\mathbf{20}(\text{MCH}^+)$ and $\mathbf{20}(\text{SP})$ isomers self-assemble into vesicles (Figure 23b). The $\mathbf{20}(\text{MCH}^+)$ isomer formed small vesicles with a constant average diameter of about 20 nm, while in contrast, the $\mathbf{20}(\text{SP})$ isomer formed larger vesicles. Upon visible light irradiation, an increase of vesicle diameter from 20 ± 3 nm ($\mathbf{20}(\text{MCH}^+)$ -vesicle) to 35 ± 4 nm ($\mathbf{20}(\text{SP})$ -vesicle) was observed in TEM images (Figure 23b) attributed to a change in head group. The metastable state of the $\mathbf{20}(\text{SP})$ -vesicle reverses following the thermal relaxation from $\mathbf{20}(\text{SP})$ to $\mathbf{20}(\text{MCH}^+)$. This study showed a reversible change in size of vesicles in water formed by a spiropyran-based amphiphile triggered by visible light.

In addition to the light-triggered transformations of self-assembled molecular amphiphiles, a multi-modal controlled assembly of a bola amphiphile was reported recently by our group.^[218] The bola amphiphile $\mathbf{21}$ based on a first-generation molecular motor core containing two carboxylic acid groups connected by alkyl linkers demonstrated light-, pH- and counter-ion controlled self-assembly in water (Figure 24a).

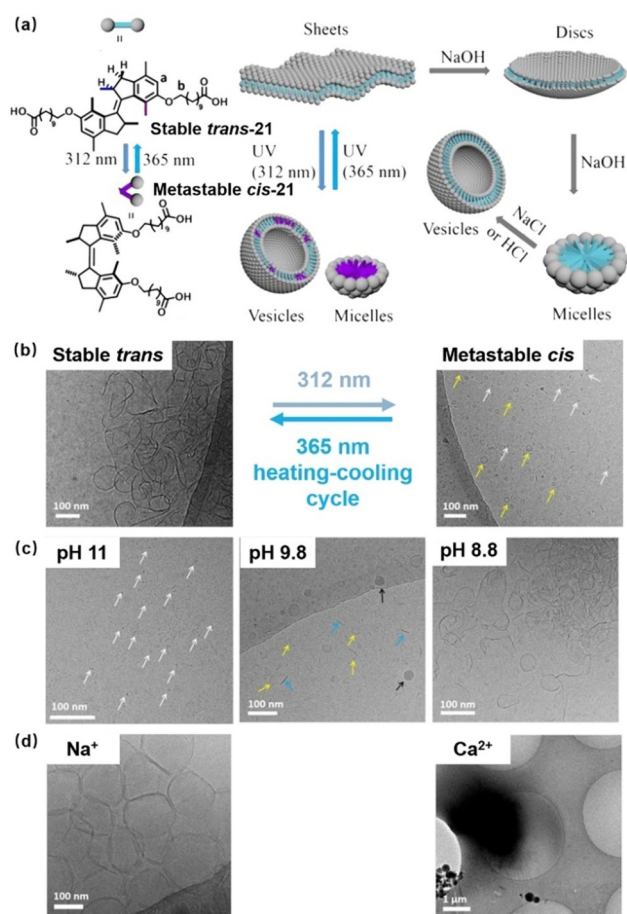


Figure 24. (a) Schematic illustration of a multi-modal control of the self-assembly of a molecular motor amphiphile $\mathbf{21}$ in aqueous media. Cryo-TEM images of (b) light-controlled, (c) pH-controlled, and (d) counter-ion controlled self-assemblies. Adapted with permission from ref. [218]. Copyright 2020, Royal Society of Chemistry.

Due to the significant geometrical changes between stable *trans*- $\mathbf{21}$ and metastable *cis*- $\mathbf{21}$, the transformation of sheet-like assemblies of stable *trans*- $\mathbf{21}$ to a mixture of sheet-like assemblies, vesicles, and micelles upon 312 nm irradiation was observed by cryo-TEM (Figure 24b). Furthermore, by tuning the pH value of the solution of stable *trans*- $\mathbf{21}$ from 11 to 8.8, modulation of its self-assembly from micelles (pH 11) to disc-like (pH 9.8) and sheet-like structures (pH 8.8) was observed (Figure 24c), which was attributed to the change of packing parameter upon protonation of stable *trans*- $\mathbf{21}$. Interestingly, the solution of stable *trans*- $\mathbf{21}$ sodium carboxylate at high pH showed vesicle structures, while macroscopic precipitates were obtained in the solution of stable *trans*- $\mathbf{21}$ calcium carboxylate, demonstrating the counter-ion effect on self-assembly structures (Figure 24d). This study provided multi-modal control over self-assembly in aqueous media. However, an extra heating-cooling cycle was needed to achieve the reversible photoresponsive assembly transformations.

Simultaneously, a novel molecular motor amphiphile $\mathbf{22}$, based on a first-generation of molecular motor core and functionalized with a hydrophobic alkyl chain and a hydrophilic quaternary ammonium moiety connected via a triethylene glycol linker, was reported by our group (Figure 25).^[157] This amphiphile showed unique dynamic photoresponsive assemblies with multiple states, resulting in the control of macroscopic foam properties in aqueous media. A reversible photoisomerization between stable *trans*- $\mathbf{22}$ and metastable *cis*- $\mathbf{22}$ by alternating 254 and 365 nm light irradiation was determined by UV-vis and NMR spectroscopy. This isomerization was accompanied by reversible transformations of self-assembled worm-like micelles to a mixture of worm-like micelles and vesicles together with a reversible switching of foaming ratio from ≈ 13 to ≈ 8 , i.e., state 1 and state 2 (Figure 25b). It is noted that this reversible assembly trans-

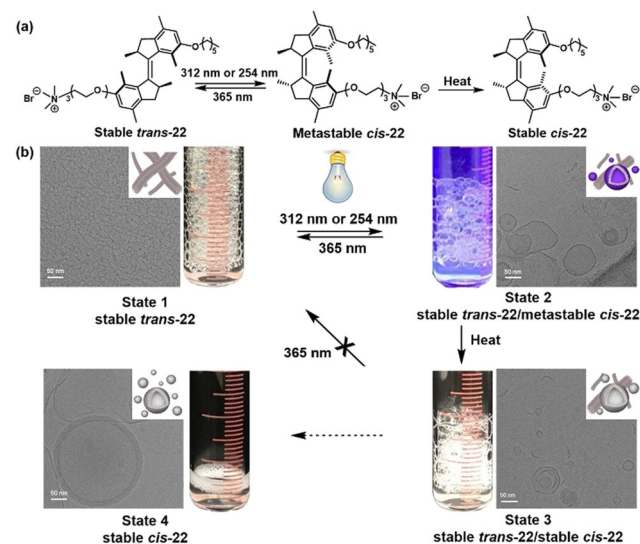


Figure 25. Schematic illustration of (a) the reversible photoisomerization and thermal helix inversion of amphiphile $\mathbf{22}$ and (b) the multi-state of macroscopic foaming processes control by selecting light/heat stimuli due to the dynamic assembly transformations. Scale bars in cryo-TEM images are 50 nm. Adapted with permission from ref. [157]. Copyright 2020, American Chemical Society.

formation was triggered by a short irradiation time of only 6 min. Additionally, with a subsequent 254 nm light irradiation and heating process, the 180° molecular rotation from stable *trans*-**22** to stable *cis*-**22** also enabled the transformation from worm-like micelles to a mixture of worm-like micelles and vesicles. However, the latter transformation cannot be switched back by 365 nm light, resulting in an irreversible change of foaming ratio from ≈ 13 to ≈ 8 (state 3, Figure 25b). By combining molecular isomerization, transformation of self-assembly, in situ surface tension and macroscopic foam properties, a correlation of amplification from molecular motion to microscopic structural transformations and macroscopic functions was established and a mechanism for the control of foam properties with multiple states was proposed. Furthermore, this system allows the unprecedented control of assembly transformations with reversibility and multi-states, without helper lipids or extra freeze-thaw cycles, providing new prospects for future soft materials.

An azobenzene amphiphile **23**, functionalized with cholesterol as hydrophobic part and tetra-alkyl-ammonium ion as hydrophilic moiety to form multilamellar vesicle by co-assembling with negatively charged SDS (Figure 26), was introduced by Wang and co-workers.^[219] The vesicles showed photoresponse through increasing the interlamellar spacing from 15.4 nm to 15.7 nm upon UV light irradiation, as confirmed by SAXS measurements. Furthermore, this co-assembly can encapsulate water-soluble rhodamine B to form stable vesicles, which was further employed into rat retina by intravitreal injection to investigate the in vivo drug delivery properties. Upon photoirradiation, a faster and effective release of rhodamine B was observed. This study illustrates the potential of such supramolecular assemblies for responsive delivery and release in aqueous conditions.

Various photoresponsive molecular amphiphile designs such as single head/single tail, double tails, or bola-amphiphilic structures, have provided dynamic self-assembled structures in aqueous media. Although specific structure design for specific assembled structures remains difficult, significant changes in the molecular configuration of photo-

responsive amphiphiles is a promising strategy for the control of assembly transformations. The representative examples of photoresponsive amphiphiles (below 1.0 wt %) discussed here shown how dramatic supramolecular assembled structure transformations in aqueous solutions can be achieved upon photoirradiation. The photoresponsive amphiphiles hold promise to be applied as novel drug carriers to provide specific drug release upon irradiation with high spatio-temporal precision.

4.2. Anisotropic self-assembly of photoresponsive molecular amphiphiles

Anisotropic three-dimensional hierarchical assembled structures are omnipresent in biological systems,^[220–225] and collagen is one of the well-known examples. Triple-stranded helices are formed by folding of three polypeptide chains, followed by assembly of the microfibrils into higher hierarchical collagen fibrils. Another illustrative example pertains to actin filaments, which provides structural stability to cells and as part of the contractile apparatus in muscle cells. The helical ribbon of actin filaments is composed of two parallel strands held together tightly by multiple supramolecular interactions, in which each strand is a linear array of a protein monomer. Inspired by natural hierarchical supramolecular assemblies, the design and manipulation of synthetic molecular amphiphiles assembling into precisely organized and anisotropic macroscopic structures have recently become an attractive field in supramolecular chemistry. At macroscopic length-scales, anisotropic three-dimensional hierarchical supramolecular structures generate exciting opportunities towards applications in regenerative biomedical materials, anisotropic actuators, electronic and optoelectronic materials, and soft robotics. In 2010, Stupp and co-workers reported a macroscopic string of bundled nanofibers of a peptide amphiphile, prepared by a shear-flow method from an aqueous solution of calcium chloride.^[226] The unidirectionally aligned nanofibers served as a scaffold for cell growth, onto which cells grew along the long axis of the macroscopic string, to be potentially applied as the next generation of tissue regenerative materials.^[227,228] Recently, the Stupp group has further demonstrated that macroscopic supramolecular assembled tubes of peptide amphiphiles could be applied as templates for the formation of anisotropically aligned thermal responsive polymers, providing anisotropic macroscopic actuations upon heating.^[229] Taking inspiration from molecular motions in muscle tissues, a photoresponsive hierarchical self-assembled structure of a cationic gemini azobenzene amphiphile **24** was developed by Liu and co-workers (Figure 27).^[230] The azobenzene amphiphile **24** assembled hierarchically from nanorods into crystalline helical twisted bundles (observed by polarized optical microscopy, POM) by organic solvent evaporation during 2 days. The resulting bundled helices (≈ 3 mm in length and ≈ 25 μm in diameter) bent towards the incident light source (302 nm light, 120 min) from an initial angle of 36° to a saturated flexion angle of 50° with an actuation speed of 1.9×10^{-3} degrees $^{-1}$, providing a millimeter length-scale anisotropic actuation based on

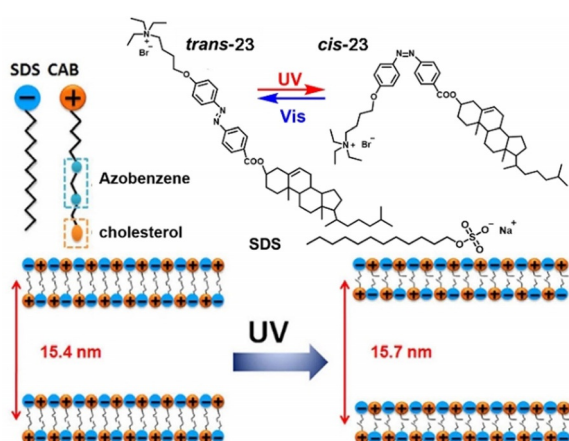


Figure 26. Schematic illustration of photoisomerization of amphiphile **23** and the corresponding increase of interlamellar spacing in the multilamellar vesicle. Adapted with permission from ref. [219]. Copyright 2017, Macmillan Publishers Limited, part of Springer Nature.

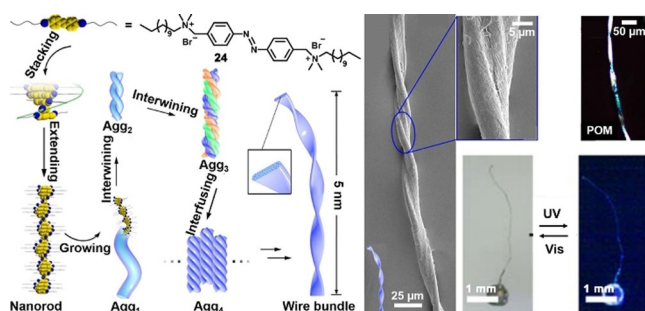


Figure 27. Schematic illustration of the hierarchical self-assembled structures of **24**. Adapted with permission from ref. [230]. Copyright 2015, Macmillan Publishers Limited, part of Springer Nature.

modulation of the supramolecular polymer interactions via photoswitching of the azobenzene amphiphile **24**. Although actuation over various length scales in a supramolecular system was achieved, a clear mechanistic understanding of the actuation mechanism is lacking and this system operates in organic media.

Recently our group reported the first unidirectionally aligned hierarchical supramolecular structure powered by a molecular motor in aqueous media to realize a photocontrolled macroscopic muscle-like action in both water and air (Figure 28).^[231] To assemble this soft actuator, a molecular motor amphiphile **25** with a dodecyl chain formed the upper half, while two carboxyl groups linked with two alkyl moieties formed the lower half (Figure 28a,b). The highly amphiphilic nature of **25** allowed micro-phase separation and molecular ordering in aqueous media forming fibers. The photoisomerization from stable-**25** to metastable-**25** and THI from metastable-**25** to stable-**25** were studied using UV-vis and

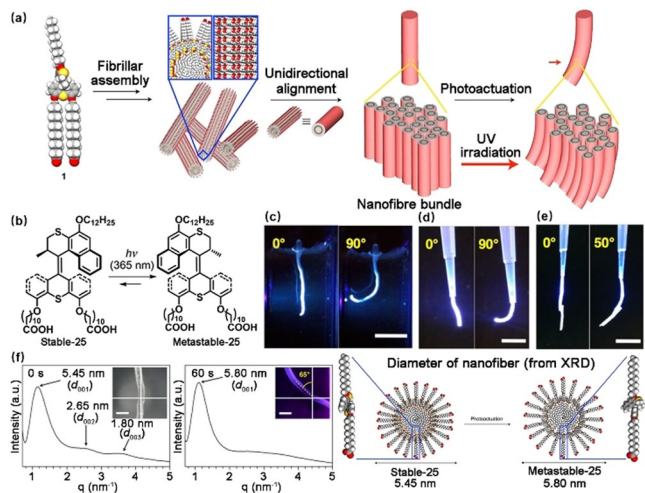


Figure 28. Schematic illustration of (a) hierarchical supramolecular assembled structures with photoactuated property of **25** and (b) isomerization processes of **25**. A nanofiber-containing solution of stable-**25** was manually drawn from a pipette into a CaCl_2 solution to achieve unidirectional alignment in bundles, generating a string that was able to bend upon exposure to UV irradiation in (c) aqueous media, (d) air without weight and (e) with 0.4 mg paper as weight, scale bar: 0.5 cm. (f) *In situ* SAXS of a stable-**25** string before and after actuation, demonstrating the photoactuation mechanism. Adapted with permission from ref. [231]. Copyright 2018, Macmillan Publishers Limited, part of Springer Nature.

^1H NMR spectroscopy, demonstrating a metastable-**25**/stable-**25** ratio of 9:1 at PSS, and a half-life of 128 h at 20 °C and 2.7 h at 50 °C for the THI step. Macroscopic strings were prepared from a nanofiber-containing solution of **25** by a shear-flow method in a calcium chloride solution, affording unidirectionally aligned structures characterized by POM and scanning electron microscope (SEM). The macroscopic strings bent towards the light source from an initial angle of 0° to a saturated flexion angle of 90° within 60 s in water (Figure 28c). Furthermore, the macroscopic string of stable-**25** could be pulled from the aqueous media and performed photoactuators in air (Figure 28d), which allowed the attachment and motion of a 0.4 mg piece of paper (Figure 28e). The photoactuation process in air allowed *in situ* SAXS measurements to exclude the scattering effects from aqueous media. According to the SAXS results (Figure 28f), a mechanism for the photoactuation was proposed involving the photoisomerization from stable-**25** to metastable-**25** resulted in an increase of excluded volume around the motor unit and disturbance of local packing arrangement in the motor amphiphiles. In the meantime, the diameter of nanofibers expanded while the total volume of the macroscopic string remained unchanged, resulting the contraction of the string at the long axis. Considering the light penetration and the thickness of the string ($\approx 300 \mu\text{m}$), a light intensity gradient enables the bending of the macroscopic string towards the incident light source. This study clearly demonstrated that the motor amphiphile assembled hierarchically in water with the individual nanofibers assembling into bundled nanofibers and, more importantly, the nanofibers were aligned unidirectionally, allowing for an effective energy conversion, accumulation, and amplification of molecular motion from the nanoscale up to macroscopic dimensions.

In this artificial muscle, the electrostatic interaction between the carboxylate groups of motor amphiphile **25** and Ca^{2+} allowed the stabilization of nanofiber of **25** and the formation of a macroscopic string. The effect of the nature of the cationic counterion on the hierarchical assembled supramolecular structure was investigated to show the dependence of the ion effect on the nanofiber formation, aggregation of nanofiber, structural order of macroscopic string, and its photoactuation speed (Figure 29).^[232] The 2D-SAXS images

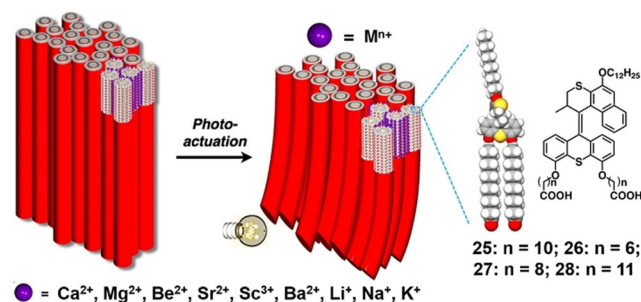


Figure 29. Schematic illustration of molecular structures of amphiphiles **25–28** with various lengths of alkyl linkers and the hierarchical organization and photoactuation process of their assembled structures by the addition of different cationic counterions. Adapted with permission from ref. [232]. Copyright 2018, American Chemical Society.

of stable-**25** macroscopic strings, prepared from a series of chloride salts, demonstrated the cationic counterion effect on the orientational order, i.e., the order of counteractions for increasing the degree of unidirectional alignment in stable-**25** macroscopic strings: $\text{Ca}^{2+} > \text{Mg}^{2+} > \text{Be}^{2+} \approx \text{Sr}^{2+} \approx \text{Sc}^{3+} > \text{Ba}^{2+} \approx \text{Li}^+ \approx \text{Na}^+ \approx \text{K}^+$. Except for tuning the orientation order, the cationic counterion also affect the actuation speed of stable-**25** macroscopic strings, i.e., the order of counteractions for accelerating actuation speed: $\text{Ca}^{2+} > \text{Mg}^{2+} > \text{Sr}^{2+} \approx \text{Sc}^{3+} > \text{Be}^{2+}$. The stable strings of **25**, prepared from solutions of BaCl_2 , LiCl , NaCl , and KCl , revealed no alignment, and no actuation was observed upon photoirradiation. The results indicated that the structural order and orientation order of the string, as well as the actuation speed, can be fine-tuned by selection of a particular metal chloride for preparing the stable-**25** macroscopic string. In addition to the counter-anion effect, the alkyl linker of motor amphiphile connecting the carboxyl group to the lower half of the motor unit was modified to various lengths (amphiphile **25–28**) to provide a systematic modification of the packing in the resultant motor amphiphile strings and their actuation functions (Figure 29). The results showed that stable-**25** was the optimal structure to allow a high structural order and a fast actuation speed. This study successfully demonstrated that the three-dimensional unidirectionally aligned hierarchical supramolecular structure and its actuation function can be controlled and modified simply by the nature of the cationic counterions, without covalent modification of the motor amphiphile.

Recently, we reported the first dual-controlled macroscopic actuation and cargo carrier from a supramolecular hierarchical assembled structure of a motor amphiphile.^[233] The motor amphiphile **29** was designed with two additional histidine moieties from **25**, which acted as the nucleation site for iron nanoparticles (FeNP) formation (Figure 30a). A macroscopic string with higher structural orientation was prepared from a combination of a nanofiber-containing solution of stable-**25** and FeNP-**29** (the nanofibers of stable-**29** in indirect contact with iron nanoparticles on the surface), which were observed in POM, SEM, and SAXS measurements. The resulting string bent towards the incident light source (365 nm light) from an initial angle of 0° to a saturated flexion angle of 90° within 25 s. Furthermore, the macroscopic string of FeNP-**29/25** was able to move towards a magnetic field within 2 s (Figure 30b), allowing for the application in a cargo transport process (Figure 30c–g). By sequential control of light/magnetic stimuli, the macroscopic string of FeNP-**29/25** could carry a piece of paper away at ≈ 2 cm distance from the original position through consecutive cargo capture, transfer, and release processes.

While both bola- and head/tail-photoresponsive molecular amphiphiles are able to build supramolecular actuators across length-scale, muscle-like functions by using external stimuli, i.e., light and a magnetic field, were achieved in water using head/tail-photoresponsive molecular amphiphiles assembled into anisotropic hierarchical supramolecular structures with controllable structural order and actuation speed. This allowed the application of cargo transport and weight lifting, and an experimental demonstration of molecular

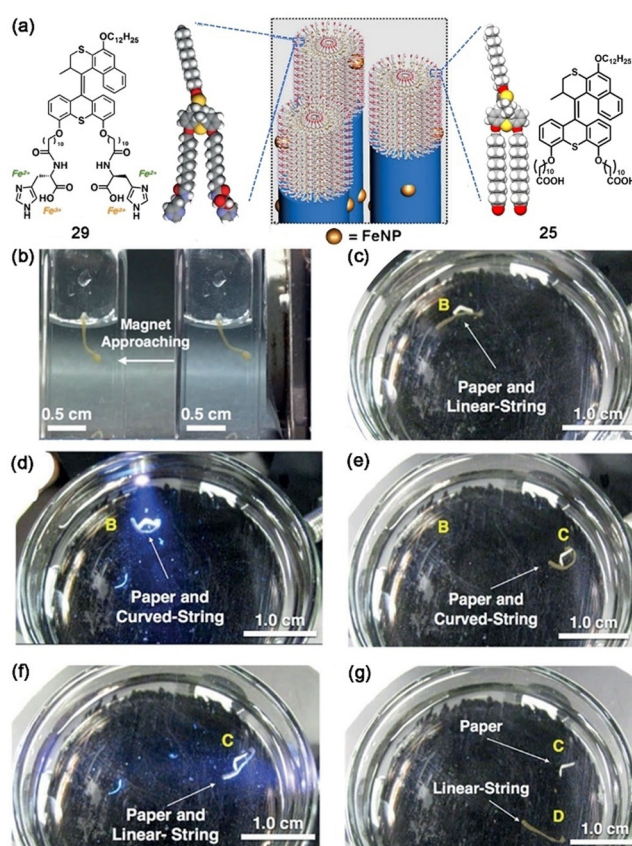


Figure 30. Schematic illustration of (a) the hierarchical organization from a combination of FeNP-**29** and **25** and (b) a FeNP-**29/25** string in a CaCl_2 solution moved towards a magnetic field from the right. Snapshots of a dual-controlled cargo process in a CaCl_2 solution: (c) a FeNP-**29/25** string in position B was (d) changed to a curved-shape upon photoirradiation, (e) carrying a piece of paper to position C guided by a magnetic field, (f) followed by changing to a linear-shape upon photoirradiation, (g) unloading the paper and moving to position D. Adapted with permission from ref. [233]. Copyright 2019, Wiley-VCH.

energy conversion, accumulation of mechanical strain of photoresponsive molecular amphiphile and amplification to macroscopic actuation using such small molecule-based supramolecular systems (for a related approach using polymer gels and molecule motors by the Giuseppone group, see^[234–236]). However, limitation so far is the slow thermal helix inversion which hinders a reversible macroscopic actuation under ambient conditions, whereas the biocompatibility of these materials remains unexplored. On the other hand, the examples discussed here unequivocally demonstrate that anisotropic hierarchical supramolecular assemblies of photoresponsive molecular amphiphiles can perform actuation in aqueous media. Arguably, the combination of photoswitches, amphiphilic structures and hierarchical supramolecular organization offers bright prospects for bridging the gap between responsive molecules and macroscopic function.

5. Summary and outlook

Supramolecular assemblies of amphiphiles in water are sustaining essential structures and functions in living organisms and are typically part of more complex adaptive and responsive systems. Taking inspiration from these biological systems and merging stimuli-responsive units with synthetic molecular amphiphiles provides fascinating opportunities towards well-defined supramolecular assembled structures which combine adaptive behavior with biomimetic functions. Compared to other external stimuli, light has the distinct advantage that it is non-invasive and can provide high spatial- and temporal control. We have discussed various approaches towards photoresponsive molecular amphiphiles, their assembly and dynamic functions, and illustrated major achievements in this emerging field of supramolecular chemistry. Addressing systems both at air–water interfaces and in aqueous solution, an overview has been presented of dynamic functions of photoresponsive amphiphiles in Gibbs monolayers, isotropic systems comprising photoresponsive amphiphiles for reversible control of assembly in water, as well as anisotropic assembly for amplification and actuation along length scales.

It is evident that the transformation of morphological states and physical parameters in both Gibbs monolayers, i.e., air–water interface, and in solution can be precisely controlled via the supramolecular assemblies of photoresponsive amphiphiles. At the molecular level, the dynamic adsorption and desorption of distinct isomers generated upon photoisomerization at air–water interfaces result in light-induced flows, e.g., Marangoni flow, allowing for macroscopic length-scale photoresponsive functions, such as photoresponsive foams, optical particle deposition, liquid marble transport, and control of crystallization. The present systems have already clearly demonstrated that Gibbs monolayers formed by photoresponsive amphiphiles at low concentration (below 1.0 wt %) allow smart responsive macroscopic functions and, for instance, responsive foams illustrate potential for the development of more environmental-friendly processing techniques.

At a relatively low concentration (below 1.0 wt %), photoresponsive amphiphiles show controllable supramolecular structures, e.g., lamellae, vesicles, nanotubes, micelles, in aqueous solution and their supramolecular structural transformations allow for instance macroscopic gel-sol processes of three-dimensional entangled networks. Furthermore, using higher concentrations of precisely designed photoresponsive amphiphiles (about 5.0 wt %) in aqueous solution, distinct nanofibers can be formed. When aligned and tightly packed into a macroscopic string, the highly oriented hierarchical supramolecular structure of bundled nanofibers allows for instance energy conversion from molecular rotations, accumulation of strain in self-assembled structures, and amplification of molecular motion into macroscopic actuation upon photoirradiation. So far, by considering the amphiphile structure, photoswitchable unit, concentration, and environmental constraints (i.e., at interfaces and in solution), several distinct supramolecular systems which show photoresponsive behavior and tunable dynamic functions in water have been realized. Despite this amazing recent progress in controlling and exploiting dynamic assembly of responsive amphiphiles, major steps are needed towards, for instance, biomedical applications, smart materials development, and industrial processes. Among the challenges of photoresponsive amphiphiles in aqueous media to be addressed are: (i) improved biocompatibility of amphiphiles, (ii) amplification of motion across length-scale, (iii) responsiveness to multiple stimuli to enhance control of functional complexity (Figure 31).

The excellent compatibility of photoresponsive amphiphiles in aqueous media has brought these systems closer to bio-related applications. However, the intrinsic cytotoxicity of highly charged amphiphiles might induce cell lysis of biological membranes. Furthermore, most of the reported photoresponsive amphiphiles are triggered by UV light, which might cause serious damage upon application in bio-systems. The toolbox of organic synthesis allows chemists to design visible or near-infrared light-driven photoresponsive amphiphiles (for recent photoswitch design, see refs. [237–256]) with reduced biotoxicity, such as using nonionic amphiphiles, exploiting the full potential of photoresponsive amphiphiles in bio-applications. Ultimately, through the encapsulation of

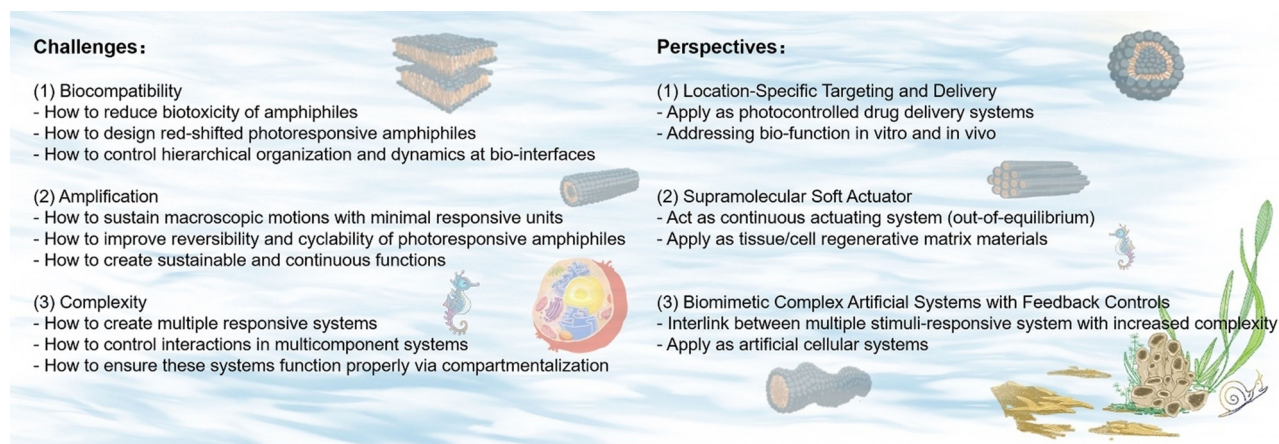


Figure 31. Outline of challenges and perspectives.

drugs by photoresponsive amphiphiles, i.e., vesicles or liposomes, stable systems for in vivo delivery with location-specific drug release taking advantage of high spatial control of light.

Although key steps in the amplification of molecular motion across length-scale to macroscopic functions, i.e., foam rupture and muscle-type actuation, have been accomplished, current applications of these systems might be hampered by the stability, repetitiveness, and cyclability of the materials. Several of the reported photoresponsive amphiphilic systems show promising reversibility, i.e., ten cycles under specified conditions, however, continuous motions or out-of-equilibrium functions remain largely unexplored. With improved biocompatibility, reversibility, and driven by visible/near-IR light, photoresponsive amphiphiles might ultimately allow supramolecular soft actuators to be potentially applied as photoresponsive tissue/cell regenerative material in vivo.

A more distant goal is the design of multiple stimuli-responsive artificial systems with feedback controls and compartmentation which might allow to develop systems mimicking cellular functions. The control of motion using light in combination with dynamic assembly provides tremendous opportunities to achieve self-regulatory and autonomous operating behavior. However, the current examples are mainly single stimulated systems, which are far from creating biomimetic complex, adaptive, and intelligent features. In this regard, through the design and synthesis of multiple responsive amphiphiles, e.g., multi-wavelength photoactivation, multiple response nature, cooperative functions, and compartmentalization, a series of sophisticated artificial systems and ultimately artificial cellular like functions might be indeed realized.

As has been illustrated here, taking advantage of the rich chemistry of molecular amphiphiles and precise control of structure and function through molecular photoswitches, fascinating opportunities arise to reversibly control assembly and function. Light and motion will guide the molecular designer, even when one has to bridge troubled waters to realize future biocompatible materials, soft actuators, and complex dynamic systems.

Acknowledgements

This work was supported financially by the China Scholarship Council (No. 201706790063 to S.Y.C.), the Croucher Foundation (Croucher Startup Allowance to F.K.C.L.), the Netherlands Organization for Scientific Research (NWO-CW), the European Research Council (ERC; Advanced Grant No. 694345 to B.L.F.), the Ministry of Education, Culture and Science (Gravitation Program No. 024.001.035). The authors thanks Qian Wang for designing and drawing the frontispiece graphic.

Conflict of interest

The authors declare no conflict of interest.

- [1] V. Degiorgio, M. Corti, *Amphiphiles: Micelles, Vesicles and Microemulsions*, North-Holland Publishing Group, Amsterdam, **1985**.
- [2] V. Degiorgio, *Europhys. News* **1985**, *16*, 9–12.
- [3] C. Domb, J. L. Lebowitz, G. Gompper, M. Schick, *Self-Assembling Amphiphilic Systems, Phase Transitions and Critical Phenomena*, Academic Press, London, **1994**.
- [4] D. Lombardo, M. A. Kiselev, S. Magazù, P. Calandra, *Adv. Condens. Matter Phys.* **2015**, 151683.
- [5] A. Sorrenti, O. Illa, R. M. Ortuño, *Chem. Soc. Rev.* **2013**, *42*, 8200–8219.
- [6] J. N. Israelachvili, D. J. Mitchell, B. W. Ninham, *J. Chem. Soc. Faraday Trans. 2* **1976**, *72*, 1525–1568.
- [7] Y. L. Chen, S. Chen, C. Frank, J. Israelachvili, *J. Colloid Interface Sci.* **1992**, *153*, 244–265.
- [8] Z. Chu, C. A. Dreiss, Y. Feng, *Chem. Soc. Rev.* **2013**, *42*, 7174–7203.
- [9] X. Zhang, C. Wang, *Chem. Soc. Rev.* **2011**, *40*, 94–101.
- [10] A. Song, J. Hao, *Curr. Opin. Colloid Interface Sci.* **2009**, *14*, 94–102.
- [11] W. Qi, L. Wu, *Polym. Int.* **2009**, *58*, 1217–1225.
- [12] A. Dolbecq, E. Dumas, C. R. Mayer, P. Mialane, *Chem. Rev.* **2010**, *110*, 6009–6048.
- [13] D. Li, P. Yin, T. Liu, *Dalton Trans.* **2012**, *41*, 2853–2861.
- [14] S. Song, R. Dong, D. Wang, A. Song, J. Hao, *Soft Matter* **2013**, *9*, 4209–4218.
- [15] C. Wang, Z. Wang, X. Zhang, *Acc. Chem. Res.* **2012**, *45*, 608–618.
- [16] S. Song, A. Song, J. Hao, *RSC Adv.* **2014**, *4*, 41864–41875.
- [17] D. Myers, *Surfactant Science and Technology*, Wiley, Hoboken, **2006**.
- [18] X. M. Liu, B. Yang, Y. L. Wang, J. Y. Wang, *Chem. Mater.* **2005**, *17*, 2792–2795.
- [19] A. Rösler, G. W. M. Vandermeulen, H. A. Klok, *Adv. Drug Delivery Rev.* **2012**, *64*, 270–279.
- [20] B. N. S. Thota, L. H. Urner, R. Haag, *Chem. Rev.* **2016**, *116*, 2079–2102.
- [21] I. C. Chen, C. Yegin, M. Zhang, M. Akbulut, *SPE J.* **2014**, *19*, 1035–1046.
- [22] J. L. Salager, A. M. Forgiarini, L. Márquez, L. Manchego, J. Bullón, *J. Surfactants Deterg.* **2013**, *16*, 631–663.
- [23] H. Hoffmann, *Adv. Mater.* **1994**, *6*, 116–129.
- [24] G. M. Whitesides, *Science* **2002**, *295*, 2418–2421.
- [25] J. S. Moore, M. L. Kraft, *Science* **2008**, *320*, 620–621.
- [26] D. T. Bong, T. D. Clark, J. R. Granja, M. Reza Ghadiri, *Angew. Chem. Int. Ed.* **2001**, *40*, 988–1011; *Angew. Chem.* **2001**, *113*, 1016–1041.
- [27] Y. Y. Luk, N. L. Abbott, *Curr. Opin. Colloid Interface Sci.* **2002**, *7*, 267–275.
- [28] T. Kato, N. Mizoshita, K. Kishimoto, *Angew. Chem. Int. Ed.* **2005**, *45*, 38–68; *Angew. Chem.* **2005**, *118*, 44–74.
- [29] G. V. Oshovsky, D. N. Reinhoudt, W. Verboom, *Angew. Chem. Int. Ed.* **2007**, *46*, 2366–2393; *Angew. Chem.* **2007**, *119*, 2418–2445.
- [30] Y. B. Lim, K. S. Moon, M. Lee, *Chem. Soc. Rev.* **2009**, *38*, 925–934.
- [31] E. Krieg, B. Rybtchinski, *Chem. Eur. J.* **2011**, *17*, 9016–9026.
- [32] H. Kim, T. Kim, M. Lee, *Acc. Chem. Res.* **2011**, *44*, 72–82.
- [33] A. C. Mendes, E. T. Baran, R. L. Reis, H. S. Azevedo, *WIREs Nanomed. Nanobiotechnol.* **2013**, *5*, 582–612.
- [34] X. Ma, H. Tian, *Acc. Chem. Res.* **2014**, *47*, 1971–1981.
- [35] X. Du, J. Zhou, B. Xu, *Chem. Asian J.* **2014**, *9*, 1446–1472.

- [36] C. Rest, R. Kandaneli, G. Fernández, *Chem. Soc. Rev.* **2015**, *44*, 2543–2572.
- [37] R. Dong, Y. Zhou, X. Huang, X. Zhu, Y. Lu, J. Shen, *Adv. Mater.* **2015**, *27*, 498–526.
- [38] F. Würthner, C. R. Saha-Möller, B. Fimmel, S. Ogi, P. Leowanawat, D. Schmidt, *Chem. Rev.* **2016**, *116*, 962–1052.
- [39] E. Krieg, M. M. C. Bastings, P. Besenius, B. Rybtchinski, *Chem. Rev.* **2016**, *116*, 2414–2477.
- [40] O. J. G. M. Goor, S. I. S. Hendrikse, P. Y. W. Dankers, E. W. Meijer, *Chem. Soc. Rev.* **2017**, *46*, 6621–6637.
- [41] K. Sato, M. P. Hendricks, L. C. Palmer, S. I. Stupp, *Chem. Soc. Rev.* **2018**, *47*, 7539–7551.
- [42] E. Krieg, A. Niazov-Elkan, E. Cohen, Y. Tsarfati, B. Rybtchinski, *Acc. Chem. Res.* **2019**, *52*, 2634–2646.
- [43] T. Aida, E. W. Meijer, *Isr. J. Chem.* **2020**, *60*, 33–47.
- [44] H. Ringsdorf, B. Schlarb, J. Venzmer, *Angew. Chem. Int. Ed. Engl.* **1988**, *27*, 113–158; *Angew. Chem.* **1988**, *100*, 117–162.
- [45] T. J. McIntosh, S. A. Simon, *Biochemistry* **1994**, *33*, 10477–10486.
- [46] S. Matile, A. Vargas Jentzsch, J. Montenegro, A. Fin, *Chem. Soc. Rev.* **2011**, *40*, 2453–2474.
- [47] J. N. Israelachvili, S. Marčelja, G. H. Roger, *Q. Rev. Biophys.* **1980**, *13*, 121–200.
- [48] P. A. Korevaar, S. J. George, A. J. Markvoort, M. M. J. Smulders, P. A. J. Hilbers, A. P. H. J. Schenning, T. F. A. de Greef, E. W. Meijer, *Nature* **2012**, *481*, 492–496.
- [49] J. Boekhoven, J. M. Poolman, C. Maity, F. Li, L. van der Mee, C. B. Minkenberg, E. Mendes, J. H. van Esch, R. Eelkema, *Nat. Chem.* **2013**, *5*, 433–437.
- [50] P. A. Korevaar, T. F. A. de Greef, E. W. Meijer, *Chem. Mater.* **2014**, *26*, 576–586.
- [51] S. Ogi, K. Sugiyasu, S. Manna, S. Samitsu, M. Takeuchi, *Nat. Chem.* **2014**, *6*, 188–195.
- [52] A. Aliprandi, M. Mauro, L. De Cola, *Nat. Chem.* **2016**, *8*, 10–15.
- [53] F. Tantakitti, J. Boekhoven, X. Wang, R. V. Kazantsev, T. Yu, J. Li, E. Zhuang, R. Zandi, J. H. Ortony, C. J. Newcomb, L. C. Palmer, G. S. Shekhawat, M. Olvera de la Cruz, G. C. Schatz, S. I. Stupp, *Nat. Mater.* **2016**, *15*, 469–476.
- [54] T. Fukui, S. Kawai, S. Fujinuma, Y. Matsushita, T. Yasuda, T. Sakurai, S. Seki, M. Takeuchi, K. Sugiyasu, *Nat. Chem.* **2017**, *9*, 493–499.
- [55] R. V. Kazantsev, A. J. Dannenhoffer, A. S. Weingarten, B. T. Phelan, B. Harutyunyan, T. Aytun, A. Narayanan, D. J. Fairfield, J. Boekhoven, H. Sai, A. Senesi, P. I. O'Dogherty, L. C. Palmer, M. J. Bedzyk, M. R. Wasielewski, S. I. Stupp, *J. Am. Chem. Soc.* **2017**, *139*, 6120–6127.
- [56] M. Wehner, F. Würthner, *Nat. Rev. Chem.* **2020**, *4*, 38–53.
- [57] A. Song, S. Dong, X. Jia, J. Hao, W. Liu, T. Liu, *Angew. Chem. Int. Ed.* **2005**, *44*, 4018–4021; *Angew. Chem.* **2005**, *117*, 4086–4089.
- [58] R. Dong, L. Zhou, D. Wang, J. Hao, *Sci. Rep.* **2013**, *3*, 1–7.
- [59] J. Singh, R. Ranganathan, S. Angayarkanny, G. Baskar, A. B. Mandal, *Langmuir* **2013**, *29*, 5734–5741.
- [60] H. Frisch, P. Besenius, *Macromol. Rapid Commun.* **2015**, *36*, 346–363.
- [61] P. Brown, T. Alan Hatton, J. Eastoe, *Curr. Opin. Colloid Interface Sci.* **2015**, *20*, 140–150.
- [62] J. Huang, Y. Yan, *Soft Matter* **2016**, *12*, 337–357.
- [63] Y. Liu, P. G. Jessop, M. Cunningham, C. A. Eckert, C. L. Liotta, *Science* **2016**, *313*, 958–960.
- [64] T. Kawai, M. Hashizume, *Stimuli-Responsive Interfaces: Fabrication and Application*, Springer Singapore, Singapore, **2016**.
- [65] N. Basílio, L. García-Río, *Curr. Opin. Colloid Interface Sci.* **2017**, *32*, 29–38.
- [66] H. Zhu, L. Shangquan, B. Shi, G. Yu, F. Huang, *Mater. Chem. Front.* **2018**, *2*, 2152–2174.
- [67] S. Santer, *J. Phys. D* **2018**, *51*, 013002.
- [68] J. Eastoe, A. Vesperinas, *Soft Matter* **2005**, *1*, 338–347.
- [69] S. Polarz, M. Kunkel, A. Donner, M. Schlötter, *Chem. Eur. J.* **2018**, *24*, 18842–18856.
- [70] R. F. Tabor, T. M. McCoy, Y. Hu, B. L. Wilkinson, *Bull. Chem. Soc. Jpn.* **2018**, *91*, 932–939.
- [71] C. Vigier-Carrière, F. Boulmedais, P. Schaaf, L. Jierry, *Angew. Chem. Int. Ed.* **2018**, *57*, 1448–1456; *Angew. Chem.* **2018**, *130*, 1462–1471.
- [72] A. R. Hirst, B. Escuder, J. F. Miravet, D. K. Smith, *Angew. Chem. Int. Ed.* **2008**, *47*, 8002–8018; *Angew. Chem.* **2008**, *120*, 8122–8139.
- [73] M. George, R. G. Weiss, *J. Am. Chem. Soc.* **2001**, *123*, 10393–10394.
- [74] X. Liu, N. L. Abbott, *J. Colloid Interface Sci.* **2009**, *339*, 1–18.
- [75] G. O. Lloyd, J. W. Steed, *Nat. Chem.* **2009**, *1*, 437–442.
- [76] P. Brown, C. P. Butts, J. Eastoe, *Soft Matter* **2013**, *9*, 2365–2374.
- [77] T. Seki, X. Lin, S. Yagai, *Asian J. Org. Chem.* **2013**, *2*, 708–724.
- [78] Q. Yan, Y. Zhao, *J. Am. Chem. Soc.* **2013**, *135*, 16300–16303.
- [79] L. Wang, Q. Li, *Chem. Soc. Rev.* **2018**, *47*, 1044–1097.
- [80] V. Balzani, A. Credi, M. Venturi, *Chem. Soc. Rev.* **2009**, *38*, 1542–1550.
- [81] C. Wang, Q. Chen, H. Xu, Z. Wang, X. Zhang, *Adv. Mater.* **2010**, *22*, 2553–2555.
- [82] S. Yagai, A. Kitamura, *Chem. Soc. Rev.* **2008**, *37*, 1520–1529.
- [83] A. D. W. Carswell, E. A. O'Rear, B. P. Grady, *J. Am. Chem. Soc.* **2003**, *125*, 14793–14800.
- [84] J. Israelachvili, H. Wennerström, *Nature* **1996**, *379*, 219–225.
- [85] P. Ball, *Chem. Rev.* **2008**, *108*, 74–108.
- [86] R. Milton, *Surfactants and Interfacial Phenomena*, Wiley, Hoboken, **1989**.
- [87] T. Kunitake, *Angew. Chem. Int. Ed. Engl.* **1992**, *31*, 709–726; *Angew. Chem.* **1992**, *104*, 692–710.
- [88] J. H. Fuhrhop, T. Wang, *Chem. Rev.* **2004**, *104*, 2901–2938.
- [89] A. Meister, M. Bastrop, S. Koschoreck, V. M. Garamus, T. Sinemus, G. Hempel, S. Drescher, B. Dobner, W. Richtering, K. Huber, A. Blume, *Langmuir* **2007**, *23*, 7715–7723.
- [90] F. M. Menger, C. A. Littau, *J. Am. Chem. Soc.* **1991**, *113*, 1451–1452.
- [91] S. Yagai, T. Karatsu, A. Kitamura, *Chem. Eur. J.* **2005**, *11*, 4054–4063.
- [92] A. Goulet-Hanssens, F. Eisenreich, S. Hecht, *Adv. Mater.* **2020**, *32*, 1905966.
- [93] M. M. Velázquez, T. Alejo, D. López-Díaz, B. Martín-García, M. D. Merchán, *Langmuir–Blodgett Methodology: A Versatile Technique to Build 2D Material Films*, InTech, **2016**.
- [94] K. Ariga, Y. Yamauchi, T. Mori, J. P. Hill, *Adv. Mater.* **2013**, *25*, 6477–6512.
- [95] E. Rogalska, R. Bilewicz, T. Brigaud, C. El Moujahid, G. Foulard, C. Portella, M. J. Stébé, *Chem. Phys. Lipids* **2000**, *105*, 71–91.
- [96] D. G. Whitten, *Acc. Chem. Res.* **1993**, *26*, 502–509.
- [97] A. Miyata, Y. Unuma, Y. Higashigaki, *Bull. Chem. Soc. Jpn.* **1991**, *64*, 1719–1725.
- [98] E. Ando, K. Moriyama, K. Arita, K. Morimoto, *Langmuir* **1990**, *6*, 1451–1454.
- [99] C. Bubeck, *Thin Solid Films* **1988**, *160*, 1–14.
- [100] H. Tachibana, Y. Yamanaka, M. Matsumoto, *J. Mater. Chem.* **2002**, *12*, 938–942.
- [101] A. Miyata, Y. Unuma, Y. Higashigaki, *Bull. Chem. Soc. Jpn.* **1993**, *66*, 993–998.
- [102] T. Yamaguchi, K. Kajikawa, H. Takezoe, A. Fukuda, *Jpn. J. Appl. Phys.* **1992**, *31*, 1160–1163.
- [103] H. Gong, J. Tang, C. Wang, M. Fan, M. Liu, *Chin. J. Chem.* **2003**, *21*, 387–391.
- [104] A. A. Kharlamov, A. V. Lyubimov, A. M. Vinogradov, *Thin Solid Films* **1994**, *244*, 962–965.

- [105] B. Song, J. Zhao, *Chin. J. Chem.* **2010**, *28*, 189–192.
- [106] O. Karthaus, M. Shimomura, M. Hioki, R. Tahara, H. Nakamura, *J. Am. Chem. Soc.* **1996**, *118*, 9174–9175.
- [107] I. Kim, J. F. Rabolt, P. Stroeve, *Colloids Surf. A* **2000**, *171*, 167–174.
- [108] T. Nakazawa, R. Azumi, H. Sakai, M. Abe, M. Matsumoto, *Langmuir* **2004**, *20*, 5439–5444.
- [109] T. Yamamoto, Y. Umemura, O. Sato, Y. Einaga, *Chem. Mater.* **2004**, *16*, 1195–1201.
- [110] E. H. G. Backus, J. M. Kuiper, J. B. F. N. Engberts, B. Poolman, M. Bonn, *J. Phys. Chem. B* **2011**, *115*, 2294–2302.
- [111] J. Cheng, P. Štacko, P. Rudolf, R. Y. N. Gengler, B. L. Feringa, *Angew. Chem. Int. Ed.* **2017**, *56*, 291–296; *Angew. Chem.* **2017**, *129*, 297–302.
- [112] A. K. Rossos, M. Katsiaflaka, J. Cai, S. M. Myers, E. Koenig, R. Bucker, S. Keskin, G. Kassier, R. Y. N. Gengler, R. J. D. Miller, R. S. Murphy, *Langmuir* **2018**, *34*, 10905–10912.
- [113] D. A. Holden, H. Ringsdorf, V. Deblauwe, G. Smets, *J. Phys. Chem.* **1984**, *88*, 716–720.
- [114] E. Ando, J. Miyazaki, K. Morimoto, H. Nakahara, K. Fukuda, *Thin Solid Films* **1985**, *133*, 21–28.
- [115] T. Seki, R. Fukuda, M. Yokoi, T. Tamaki, K. Ichimura, *Bull. Chem. Soc. Jpn.* **1996**, *69*, 2375–2381.
- [116] S. Shinkai, K. Matsuo, A. Harada, M. Osamu, *J. Chem. Soc. Perkin Trans. 2* **1982**, 1261–1265.
- [117] C. J. Drummond, S. Albers, D. N. Furlong, D. Wells, *Langmuir* **1991**, *7*, 2409–2411.
- [118] I. R. Dunkin, A. Gittinger, D. C. Sherrington, P. Whittaker, *J. Chem. Soc.* **1994**, *19*, 2245–2246.
- [119] T. Hayashita, T. Kurosawa, T. Miyata, K. Tanaka, M. Igawa, *Colloid Polym. Sci.* **1994**, *272*, 1611–1619.
- [120] L. Yang, N. Takisawa, T. Hayashita, K. Shirahama, *J. Phys. Chem.* **1995**, *99*, 8799–8803.
- [121] I. R. Dunkin, A. Gittinger, D. C. Sherrington, P. Whittaker, *J. Chem. Soc. Perkin Trans. 2* **1996**, 1837–1842.
- [122] H. C. Kang, B. M. Lee, J. Yoon, M. Yoon, *J. Colloid Interface Sci.* **2000**, *231*, 255–264.
- [123] J. Eastoe, M. S. Dominguez, P. Wyatt, A. Beeby, R. K. Heenan, *Langmuir* **2002**, *18*, 7837–7844.
- [124] T. Shang, K. A. Smith, T. A. Hatton, *Langmuir* **2003**, *19*, 10764–10773.
- [125] K. Sakai, Y. Imaizumi, T. Oguchi, H. Sakai, M. Abe, *Langmuir* **2010**, *26*, 9283–9288.
- [126] J. Y. Shin, N. L. Abbott, *Langmuir* **1999**, *15*, 4404–4410.
- [127] B. A. Ciccirelli, T. A. Hatton, K. A. Smith, *Langmuir* **2007**, *23*, 4753–4764.
- [128] W. D. Harkins, H. F. Jordan, *J. Am. Chem. Soc.* **1930**, *52*, 1751–1772.
- [129] E. Chevallier, A. Mamane, H. A. Stone, C. Tribet, F. Lequeux, C. Monteux, *Soft Matter* **2011**, *7*, 7866–7874.
- [130] E. Chevallier, C. Monteux, F. Lequeux, C. Tribet, *Langmuir* **2012**, *28*, 2308–2312.
- [131] E. Chevallier, A. Saint-Jalmes, I. Cantat, F. Lequeux, C. Monteux, *Soft Matter* **2013**, *9*, 7054–7060.
- [132] A. Mamane, E. Chevallier, L. Olanier, F. Lequeux, C. Monteux, *Soft Matter* **2017**, *13*, 1299–1305.
- [133] J. Jiang, Y. Ma, Z. Cui, *Colloids Surf. A* **2017**, *513*, 287–291.
- [134] L. Lei, D. Xie, B. Song, J. Jiang, X. Pei, Z. Cui, *Langmuir* **2017**, *33*, 7908–7916.
- [135] S. Shi, T. Yin, W. Shen, *RSC Adv.* **2016**, *6*, 93621–93625.
- [136] S. Chen, C. Wang, Y. Yin, K. Chen, *RSC Adv.* **2016**, *6*, 60138–60144.
- [137] S. Chen, W. Zhang, C. Wang, S. Sun, *Green Chem.* **2016**, *18*, 3972–3980.
- [138] S. Chen, Y. Zhang, K. Chen, Y. Yin, C. Wang, *ACS Appl. Mater. Interfaces* **2017**, *9*, 13778–13784.
- [139] L. Fei, F. Ge, Y. Yin, C. Wang, *Colloids Surf. A* **2019**, *560*, 366–375.
- [140] S. Chen, L. Fei, F. Ge, C. Wang, *Soft Matter* **2019**, *15*, 8313–8319.
- [141] S. Chen, L. Fei, F. Ge, J. Liu, Y. Yin, C. Wang, *J. Cleaner Prod.* **2020**, *243*, 118504.
- [142] X. Jiang, Q. Guo, H. Li, J. Jiang, Y. Chen, T. Xie, *Colloids Surf. A* **2017**, *535*, 201–205.
- [143] X. Jiang, Q. Guo, Y. He, H. Li, T. Xie, *Colloids Surf. A* **2018**, *553*, 218–224.
- [144] A. Diguët, R. Guillermic, N. Magome, A. Saint-Jalmes, Y. Chen, K. Yoshikawa, D. Baigl, *Angew. Chem. Int. Ed.* **2009**, *48*, 9281–9284; *Angew. Chem.* **2009**, *121*, 9445–9448.
- [145] D. Baigl, *Lab Chip* **2012**, *12*, 3637–3653.
- [146] S. N. Varanakkottu, M. Anyfantakis, M. Morel, S. Rudiuk, D. Baigl, *Nano Lett.* **2016**, *16*, 644–650.
- [147] C. Lv, S. N. Varanakkottu, T. Baier, S. Hardt, *Nano Lett.* **2018**, *18*, 6924–6930.
- [148] N. Kavokine, M. Anyfantakis, M. Morel, S. Rudiuk, T. Bickel, D. Baigl, *Angew. Chem. Int. Ed.* **2016**, *55*, 11183–11187; *Angew. Chem.* **2016**, *128*, 11349–11353.
- [149] J. Vialetto, M. Anyfantakis, S. Rudiuk, M. Morel, D. Baigl, *Angew. Chem. Int. Ed.* **2019**, *58*, 9145–9149; *Angew. Chem.* **2019**, *131*, 9243–9247.
- [150] M. Schnurbus, L. Stricker, B. J. Ravoo, B. Braunschweig, *Langmuir* **2018**, *34*, 6028–6035.
- [151] C. Honnigfort, R. A. Campbell, J. Droste, P. Gutfreund, M. R. Hansen, B. J. Ravoo, B. Braunschweig, *Chem. Sci.* **2020**, *11*, 2085–2092.
- [152] H. Sakai, H. Ebana, K. Sakai, K. Tsuchiya, T. Ohkubo, M. Abe, *J. Colloid Interface Sci.* **2007**, *316*, 1027–1030.
- [153] J. G. S. Moo, S. Presolski, M. Pumera, *ACS Nano* **2016**, *10*, 3543–3552.
- [154] M. Schnurbus, M. Kabat, E. Jarek, M. Krzan, P. Warszynski, B. Braunschweig, *Langmuir* **2020**, *36*, 6871–6879.
- [155] B. V. Zhmud, F. Tiberg, J. Kizling, *Langmuir* **2000**, *16*, 2557–2565.
- [156] D. Beneventi, B. Carre, A. Gandini, *Colloids Surf. A* **2001**, *189*, 65–73.
- [157] S. Chen, F. K. C. Leung, M. C. A. Stuart, C. Wang, B. L. Feringa, *J. Am. Chem. Soc.* **2020**, *142*, 10163–10172.
- [158] R. Nagarajan, *Langmuir* **2002**, *18*, 31–38.
- [159] J. Li, M. Zhao, H. Zhou, H. Gao, L. Zheng, *Soft Matter* **2012**, *8*, 7858–7864.
- [160] D. Wang, G. Wei, R. Dong, J. Hao, *Chem. Eur. J.* **2013**, *19*, 8253–8260.
- [161] R. F. Tabor, D. D. Tan, S. S. Han, S. A. Young, Z. L. E. Seeger, M. J. Pottage, C. J. Garvey, B. L. Wilkinson, *Chem. Eur. J.* **2014**, *20*, 13881–13884.
- [162] Y. Tu, Q. Chen, Y. Shang, H. Teng, H. Liu, *Langmuir* **2019**, *35*, 4634–4645.
- [163] A. L. Fameau, A. Arnould, M. Lehmann, R. Von Klitzing, *Chem. Commun.* **2015**, *51*, 2907–2910.
- [164] K. Jia, J. Hu, J. Dong, X. Li, *J. Colloid Interface Sci.* **2016**, *477*, 156–165.
- [165] C. Blayo, J. E. Houston, S. M. King, R. C. Evans, *Langmuir* **2018**, *34*, 10123–10134.
- [166] T. Shimizu, M. Masuda, H. Minamikawa, *Chem. Rev.* **2005**, *105*, 1401–1443.
- [167] J. J. D. de Jong, L. N. Lucas, R. M. Kellogg, J. H. van Esch, B. L. Feringa, *Science* **2004**, *304*, 278–281.
- [168] R. Eelkema, B. L. Feringa, *Org. Biomol. Chem.* **2006**, *4*, 3729–3745.
- [169] J. J. D. de Jong, P. van Rijn, T. D. Tiemersma-Wegeman, L. N. Lucas, W. R. Browne, R. M. Kellogg, K. Uchida, J. H. van Esch, B. L. Feringa, *Tetrahedron* **2008**, *64*, 8324–8335.

- [170] N. Katsonis, E. Lacaze, B. L. Feringa, *J. Mater. Chem.* **2008**, *18*, 2065–2073.
- [171] T. G. Barclay, K. Constantopoulos, J. Matisons, *Chem. Rev.* **2014**, *114*, 10217–10291.
- [172] D. J. van Dijken, J. M. Beierle, M. C. A. Stuart, W. Szymański, W. R. Browne, B. L. Feringa, *Angew. Chem. Int. Ed.* **2014**, *53*, 5073–5077; *Angew. Chem.* **2014**, *126*, 5173–5177.
- [173] M. Liu, L. Zhang, T. Wang, *Chem. Rev.* **2015**, *115*, 7304–7397.
- [174] T. Muraoka, H. Cui, S. I. Stupp, *J. Am. Chem. Soc.* **2008**, *130*, 2946–2947.
- [175] T. Muraoka, C. Y. Koh, H. Cui, S. I. Stupp, *Angew. Chem. Int. Ed.* **2009**, *48*, 5946–5949; *Angew. Chem.* **2009**, *121*, 6060–6063.
- [176] S. E. Paramonov, H. W. Jun, J. D. Hartgerink, *J. Am. Chem. Soc.* **2006**, *128*, 7291–7298.
- [177] A. C. Coleman, J. M. Beierle, M. C. A. Stuart, B. Maciá, G. Caroli, J. T. Mika, D. J. van Dijken, J. Chen, W. R. Browne, B. L. Feringa, *Nat. Nanotechnol.* **2011**, *6*, 547–552.
- [178] P. M. Erne, L. S. van Bezouwen, P. Štacko, D. J. van Dijken, J. Chen, M. C. A. Stuart, E. J. Boekema, B. L. Feringa, *Angew. Chem. Int. Ed.* **2015**, *54*, 15122–15127; *Angew. Chem.* **2015**, *127*, 15337–15342.
- [179] Y. Sun, Y. Ji, H. Yu, D. Wang, M. Cao, J. Wang, *RSC Adv.* **2016**, *6*, 81245–81249.
- [180] D. Wang, X. Hou, B. Ma, Y. Sun, J. Wang, *Soft Matter* **2017**, *13*, 6700–6708.
- [181] G. J. Wang, J. B. F. N. Engberts, *Langmuir* **1994**, *10*, 2583–2587.
- [182] R. T. Buwalda, J. M. Jonker, J. B. F. N. Engberts, *Langmuir* **1999**, *15*, 1083–1089.
- [183] R. T. Buwalda, J. B. F. N. Engberts, *Langmuir* **2001**, *17*, 1054–1059.
- [184] R. T. Buwalda, M. C. A. Stuart, J. B. F. N. Engberts, *Langmuir* **2002**, *18*, 6507–6512.
- [185] L. S. Li, H. Jiang, B. W. Messmore, S. R. Bull, S. I. Stupp, *Angew. Chem. Int. Ed.* **2007**, *46*, 5873–5876; *Angew. Chem.* **2007**, *119*, 5977–5980.
- [186] X. Song, J. Perlstein, D. G. Whitten, *J. Am. Chem. Soc.* **1997**, *119*, 9144–9159.
- [187] H. Sakai, A. Matsumura, S. Yokoyama, T. Saji, M. Abe, *J. Phys. Chem. B* **1999**, *103*, 10737–10740.
- [188] R. F. Khairutdinov, J. K. Hurst, *Langmuir* **2004**, *20*, 1781–1785.
- [189] C. T. Lee, K. A. Smith, T. A. Hatton, *Macromolecules* **2004**, *37*, 5397–5405.
- [190] M. Bonini, D. Berti, J. M. Di Meglio, M. Almgren, J. Teixeira, P. Baglioni, *Soft Matter* **2005**, *1*, 444–454.
- [191] D. Faure, J. Gravier, T. Labrot, B. Desbat, R. Oda, D. M. Bassani, *Chem. Commun.* **2005**, *16*, 1167–1169.
- [192] F. P. Hubbard, G. Santonicola, E. W. Kaler, N. L. Abbott, *Langmuir* **2005**, *21*, 6131–6136.
- [193] T. Shang, K. A. Smith, T. A. Hatton, *Langmuir* **2006**, *22*, 1436–1442.
- [194] F. P. Hubbard, N. L. Abbott, *Langmuir* **2007**, *23*, 4819–4829.
- [195] H. Sakai, Y. Orihara, H. Kodashima, A. Matsumura, T. Ohkubo, K. Tsuchiya, M. Abe, *J. Am. Chem. Soc.* **2005**, *127*, 13454–13455.
- [196] C. Alvarez-Lorenzo, L. Bromberg, A. Concheiro, *Photochem. Photobiol.* **2009**, *85*, 848–860.
- [197] N. Fomina, J. Sankaranarayanan, A. Almutairi, *Adv. Drug Delivery Rev.* **2012**, *64*, 1005–1020.
- [198] Y. Lin, X. Cheng, Y. Qiao, C. Yu, Z. Li, Y. Yan, J. Huang, *Soft Matter* **2010**, *6*, 902–908.
- [199] Y. Bi, H. Wei, Q. Hu, W. Xu, Y. Gong, L. Yu, *Langmuir* **2015**, *31*, 3789–3798.
- [200] R. Giernoth, *Angew. Chem. Int. Ed.* **2010**, *49*, 2834–2839; *Angew. Chem.* **2010**, *122*, 2896–2901.
- [201] S. S. Dandpat, M. Sarkar, *Phys. Chem. Chem. Phys.* **2015**, *17*, 13992–14002.
- [202] H. Tamura, Y. Shinohara, T. Arai, *Chem. Lett.* **2010**, *39*, 240–241.
- [203] S. Zhang, S. Liu, Q. Zhang, Y. Deng, *Chem. Commun.* **2011**, *47*, 6641–6643.
- [204] J. Avó, L. Cunha-Silva, J. C. Lima, A. Jorge Parola, *Org. Lett.* **2014**, *16*, 2582–2585.
- [205] J. Yang, H. Wang, J. Wang, Y. Zhang, Z. Guo, *Chem. Commun.* **2014**, *50*, 14979–14982.
- [206] S. Shi, T. Yin, X. Tao, W. Shen, *RSC Adv.* **2015**, *5*, 75806–75809.
- [207] J. Yang, H. Wang, J. Wang, X. Guo, Y. Zhang, *RSC Adv.* **2015**, *5*, 96305–96312.
- [208] A. Wu, F. Lu, P. Sun, X. Gao, L. Shi, L. Zheng, *Langmuir* **2016**, *32*, 8163–8170.
- [209] Z. Li, H. Wang, M. Chu, P. Guan, Y. Zhao, Y. Zhao, J. Wang, *RSC Adv.* **2017**, *7*, 44688–44695.
- [210] R. F. Tabor, M. J. Pottage, C. J. Garvey, B. L. Wilkinson, *Chem. Commun.* **2015**, *51*, 5509–5512.
- [211] E. A. Kelly, J. E. Houston, R. C. Evans, *Soft Matter* **2019**, *15*, 1253–1259.
- [212] R. Lund, G. Brun, E. Chevallier, T. Narayanan, C. Tribet, *Langmuir* **2016**, *32*, 2539–2548.
- [213] B. Song, Y. Hu, J. Zhao, *J. Colloid Interface Sci.* **2009**, *333*, 820–822.
- [214] D. Zhang, X. Lu, Y. Li, G. Wang, Y. Chen, J. Jiang, *Colloids Surf. A* **2018**, *543*, 155–162.
- [215] T. Hirose, K. Matsuda, M. Irie, *J. Org. Chem.* **2006**, *71*, 7499–7508.
- [216] D. J. van Dijken, J. Chen, M. C. A. Stuart, L. Hou, B. L. Feringa, *J. Am. Chem. Soc.* **2016**, *138*, 660–669.
- [217] S. Kwangmettattam, T. Kudernac, *Chem. Commun.* **2018**, *54*, 5311–5314.
- [218] F. Xu, L. Pfeifer, M. C. A. Stuart, F. K. C. Leung, B. L. Feringa, *Chem. Commun.* **2020**, *56*, 7451–7454.
- [219] S. Geng, Y. Wang, L. Wang, T. Kouyama, T. Gotoh, S. Wada, J. Y. Wang, *Sci. Rep.* **2017**, *7*, 1–13.
- [220] N. S. Simmons, E. R. Blout, *Biophys. J.* **1960**, *1*, 55–62.
- [221] T. Lino, *J. Supramol. Struct.* **1974**, *2*, 372–384.
- [222] D. J. Prockop, A. Fertala, *J. Struct. Biol.* **1998**, *122*, 111–118.
- [223] C. J. Tsai, B. Ma, S. Kumar, H. Wolfson, R. Nussinov, *Crit. Rev. Biochem. Mol. Biol.* **2001**, *36*, 399–433.
- [224] D. A. Fletcher, R. D. Mullins, *Nature* **2010**, *463*, 485–492.
- [225] F. Huber, J. Schnauß, S. Röncke, P. Rauch, K. Müller, C. Fütterer, J. Käs, *Adv. Phys.* **2013**, *62*, 1–112.
- [226] S. Zhang, M. A. Greenfield, A. Mata, L. C. Palmer, R. Bitton, J. R. Mantei, C. Aparicio, M. O. De La Cruz, S. I. Stupp, *Nat. Mater.* **2010**, *9*, 594–601.
- [227] N. L. Angeloni, C. W. Bond, Y. Tang, D. A. Harrington, S. Zhang, S. I. Stupp, K. E. McKenna, C. A. Podlasek, *Biomaterials* **2011**, *32*, 1091–1101.
- [228] M. T. McClendon, S. I. Stupp, *Biomaterials* **2012**, *33*, 5713–5722.
- [229] S. M. Chin, C. V. Synatschke, S. Liu, R. J. Nap, N. A. Sather, Q. Wang, Z. Álvarez, A. N. Edelbrock, T. Fyrner, L. C. Palmer, I. Szleifer, M. Olvera de la Cruz, S. I. Stupp, *Nat. Commun.* **2018**, *9*, 1–11.
- [230] Y. Sheng, Q. Chen, J. Yao, Y. Wang, H. Liu, *Sci. Rep.* **2015**, *5*, 7791.
- [231] J. Chen, F. K. C. Leung, M. C. A. Stuart, T. Kajitani, T. Fukushima, E. van der Giessen, B. L. Feringa, *Nat. Chem.* **2018**, *10*, 132–138.
- [232] F. K. C. Leung, T. van den Enk, T. Kajitani, J. Chen, M. C. A. Stuart, J. Kuipers, T. Fukushima, B. L. Feringa, *J. Am. Chem. Soc.* **2018**, *140*, 17724–17733.
- [233] F. K. C. Leung, T. Kajitani, M. C. A. Stuart, T. Fukushima, B. L. Feringa, *Angew. Chem. Int. Ed.* **2019**, *58*, 10985–10989; *Angew. Chem.* **2019**, *131*, 11101–11105.

- [234] Q. Li, G. Fuks, E. Moulin, M. Maaloum, M. Rawiso, I. Kulic, J. T. Foy, N. Giuseppone, *Nat. Nanotechnol.* **2015**, *10*, 161–165.
- [235] J. T. Foy, Q. Li, A. Goujon, J. R. Colard-Itté, G. Fuks, E. Moulin, O. Schiffmann, D. Dattler, D. P. Funeriu, N. Giuseppone, *Nat. Nanotechnol.* **2017**, *12*, 540–545.
- [236] A. Goujon, G. Mariani, T. Lang, E. Moulin, M. Rawiso, E. Buhler, N. Giuseppone, *J. Am. Chem. Soc.* **2017**, *139*, 4923–4928.
- [237] M. J. Hansen, M. M. Lerch, W. Szymanski, B. L. Feringa, *Angew. Chem. Int. Ed.* **2016**, *55*, 13514–13518; *Angew. Chem.* **2016**, *128*, 13712–13716.
- [238] M. Wegener, M. J. Hansen, A. J. M. Driessen, W. Szymanski, B. L. Feringa, *J. Am. Chem. Soc.* **2017**, *139*, 17979–17986.
- [239] M. Dong, A. Babalhavaeji, C. V. Collins, K. Jarrah, O. Sadovski, Q. Dai, G. A. Woolley, *J. Am. Chem. Soc.* **2017**, *139*, 13483–13486.
- [240] C. Y. Huang, A. Bonasera, L. Hristov, Y. Garmshausen, B. M. Schmidt, D. Jacquemin, S. Hecht, *J. Am. Chem. Soc.* **2017**, *139*, 15205–15211.
- [241] H. Xi, Z. Zhang, W. Zhang, M. Li, C. Lian, Q. Luo, H. Tian, W. H. Zhu, *J. Am. Chem. Soc.* **2019**, *141*, 18467–18474.
- [242] M. Jacquet, L. M. Uriarte, F. Lafalet, M. Boggio-Pasqua, M. Sliwa, F. Loiseau, E. Saint-Aman, S. Cobo, G. Royal, *J. Phys. Chem. Lett.* **2020**, *11*, 2682–2688.
- [243] D. Roke, M. Sen, W. Danowski, S. J. Wezenberg, B. L. Feringa, *J. Am. Chem. Soc.* **2019**, *141*, 7622–7627.
- [244] J. R. Hemmer, S. O. Poelma, N. Treat, Z. A. Page, N. D. Dolinski, Y. J. Diaz, W. Tomlinson, K. D. Clark, J. P. Hooper, C. Hawker, J. Read de Alaniz, *J. Am. Chem. Soc.* **2016**, *138*, 13960–13966.
- [245] M. M. Lerch, W. Szymański, B. L. Feringa, *Chem. Soc. Rev.* **2018**, *47*, 1910–1937.
- [246] M. M. Lerch, S. J. Wezenberg, W. Szymanski, B. L. Feringa, *J. Am. Chem. Soc.* **2016**, *138*, 6344–6347.
- [247] M. M. Lerch, M. J. Hansen, W. A. Velema, W. Szymanski, B. L. Feringa, *Nat. Commun.* **2016**, *7*, 1–10.
- [248] M. M. Lerch, M. Di Donato, A. D. Laurent, M. Medved', A. Iagatti, L. Bussotti, A. Lapini, W. J. Buma, P. Foggi, W. Szymański, B. L. Feringa, *Angew. Chem. Int. Ed.* **2018**, *57*, 8063–8068; *Angew. Chem.* **2018**, *130*, 8195–8200.
- [249] T. van Leeuwen, J. Pol, D. Roke, S. J. Wezenberg, B. L. Feringa, *Org. Lett.* **2017**, *19*, 1402–1405.
- [250] L. Pfeifer, M. Scherübl, M. Fellert, W. Danowski, J. Cheng, J. Pol, B. L. Feringa, *Chem. Sci.* **2019**, *10*, 8768–8773.
- [251] S. Samanta, A. Babalhavaeji, M. X. Dong, G. A. Woolley, *Angew. Chem. Int. Ed.* **2013**, *52*, 14127–14130; *Angew. Chem.* **2013**, *125*, 14377–14380.
- [252] S. Samanta, A. A. Beharry, O. Sadovski, T. M. McCormick, A. Babalhavaeji, V. Tropepe, G. A. Woolley, *J. Am. Chem. Soc.* **2013**, *135*, 9777–9784.
- [253] Y. Yang, R. P. Hughes, I. Aprahamian, *J. Am. Chem. Soc.* **2014**, *136*, 13190–13193.
- [254] D. Bléger, S. Hecht, *Angew. Chem. Int. Ed.* **2015**, *54*, 11338–11349; *Angew. Chem.* **2015**, *127*, 11494–11506.
- [255] M. Dong, A. Babalhavaeji, S. Samanta, A. A. Beharry, G. A. Woolley, *Acc. Chem. Res.* **2015**, *48*, 2662–2670.
- [256] D. B. Konrad, J. A. Frank, D. Trauner, *Chem. Eur. J.* **2016**, *22*, 4364–4368.

Manuscript received: May 29, 2020

Accepted manuscript online: September 16, 2020

Version of record online: February 24, 2021